AD NUMBER

AD480898

NEW LIMITATION CHANGE

TO

Approved for public release, distribution unlimited

FROM

Distribution authorized to U.S. Gov't. agencies and their contractors; Administrative/Operational use; 1963. Other requests shall be referred to Naval Postgraduate School, Montery CA.

AUTHORITY

USNPS ltr 21 Apr 1972

1963

Duplicate

UNITED STATES
NAVAL POSTGRADUATE SCHOOL

THESIS

SIGNAL AND NOISE ANALYSIS
AND
PERFORMANCE CRITERIA
FOR A
QUANTIZED FREQUENCY MODULATION SYSTEM

by

Walter R. Flowers

1963

SIGNAL AND NOISE ANALYSIS
AND
PERFORMANCE CRITERIA
FOR A
QUANTIZED FREQUENCY MODULATION SYSTEM

* * * * *

Walter R. Flowers

SIGNAL AND NOISE ANALYSIS

AND

PERFORMANCE CRITERIA

FOR A

QUANTIZED FREQUENCY MODULATION SYSTEM

by

Walter R. Flowers

Lieutenant, United States Navy

Submitted in partial fulfillment of
the requirements for the degree of

MASTER OF SCIENCE

IN

ENGINEERING ELECTRONICS

United States Naval Postgraduate School
Monterey, California

1 9 6 3

SIGNAL AND NOISE ANALYSIS

AND

PERFORMANCE CRITERIA

FOR A

QUANTIZED FREQUENCY MODULATION SYSTEM

by

Walter R. Flowers

This work is accepted as fulfilling

the thesis requirements for the degree of

MASTER OF SCIENCE

IN

ENGINEERING ELECTRONICS

from the

United States Naval Postgraduate School

Faculty Adviser

Faculty Adviser

Chairman
Department of Electronics

Approved:

Academic Dean

ABSTRACT

Quantized Frequency Modulation is one of the various methods used to reduce the effects of multipath propagation of high frequency radio waves. The modulation technique is described, and a signal and noise analysis is made resulting in a theoretical maximum performance criteria. A comparison is made with the performance of various configurations of the system demodulator.

The author wishes to express appreciation to Mr. G. L. Evans of the Communication Division of Hughes Aircraft Company for his assistance and encouragement.

Also the writer wishes to acknowledge the direction and instruction given by Professor Mitchel L. Cotton of the Digital Control Laboratory, U. S. Naval Postgraduate School.

TABLE OF CONTENTS

LIST OF ILLUSTRATIONS

1. Introduction.

It has long been recognized that reliability in high frequency radio communications is limited not so much by the power which can be radiated by an antenna as it is by the destructive vectoral addition of signals arriving at the receiver. The signals which are added vectorially may be delayed replicas or may be parts of two different symbols. In both cases the effect is the result of the delays in multipath propagation. The first case is selective fading, and the second case is intersymbol interference.

There have been many schemes devised in attempts to reduce the effects of multipath propagation phenomena. Several forms of diversity reception including time diversity, space diversity and frequency diversity each designed to isolate one of the incoming signals, and various combining techniques have been used. /1/ Other schemes include the use of single sideband /2/ and synchronous detection. /3/

Probably the most advanced technique in combatting multipath effects is the "Rake" system. /4/ This system uses a cross correlation detection scheme, coupled with a method for isolating the signal from each path, and then combines the signals from each path in nearly optimum proportions.

All these schemes have their own advantages and disadvantages. Usually the best results are obtained by

those schemes requiring large antennas or complex equipment, or large land areas. Other schemes of less complexity can expect less increase in reliability.

The modulation scheme analyzed in this paper is one designed to operate within the bandwidth of one single-sideband voice channel of 3 K.C. Also a minimum size and weight limitation is imposed which precludes large antennas or space diversity techniques. Instead a type of frequency diversity is employed which allows the transmitter to operate at a nearly constant power output. A coded pulse is used for both the "mark" and "space", and a delay line summer is used to add coherently the output pulses.

The modulation scheme will be described and related to the principles of communication theory. A signal and noise analysis will be made on the system to predict error rates for various signal to noise power ratios.

The methods and results of laboratory testing of the demodulator under various signal to noise ratios will be presented. Comparisons will be made between the predicted error rates and the actual error rates.

2. System Operation.

This section includes a description of the basic modulation scheme and the method used for demodulation. The principles of communication theory which this system implements are emphasized where employed.

2.1 Basic modulation scheme.

Quantized Frequency Modulation (QFM) is the name given to the modulation scheme developed by the Communications Division of Hughes Aircraft Company. This scheme was devised in an effort to reduce the effects of multipath fading on the reliability of teletype or mark-space communications systems.

A combination of several techniques is applied, and these techniques will be described in later sections.

The tapped delay line approximation to the matched filter is used in this system as follows.

A combination of short pulses and frequency stepping is used to reduce the effects of intersymbol interference and selective fading respectively. The short pulses are spaced at each frequency to allow time for the path delays to die out. But upon detection these pulses are added coherently by means of the tapped delay line. Fig. 1 is an idealized graphical representation of the signal transmitted.

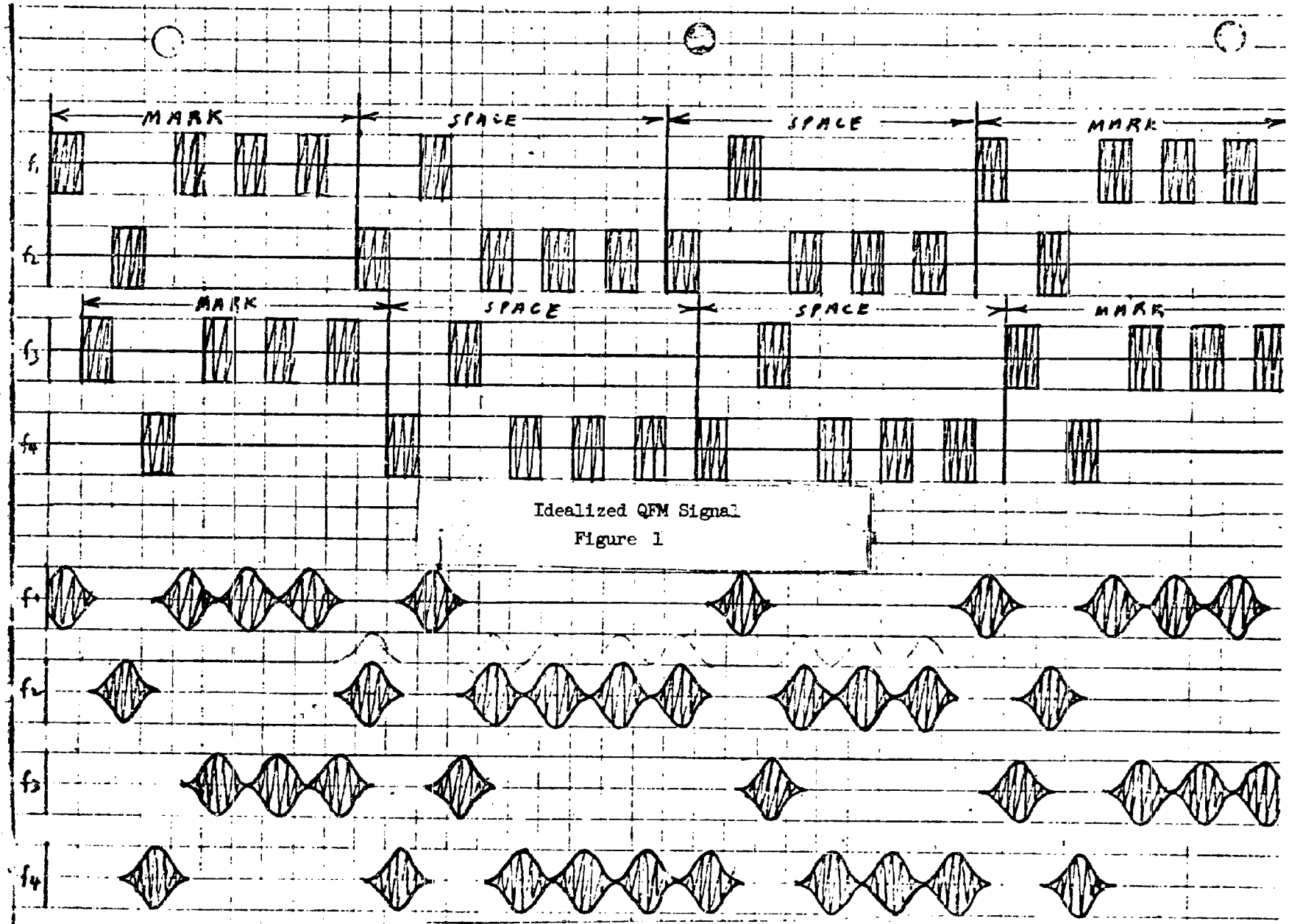

Idealized QFM Signal

Figure 1

Actual QFM Signal

Figure 2

This is the modulation on a carrier. Notice that there is uninterrupted modulation of the carrier, and hence the output power is constant. In order to contain the modulation within a 3KC bandwidth the pulses are shaped to approximately a cosine squared shape. An example of the actual shaped pulses is shown in Fig. 2 for Mark--Space--Space--Mark as before.

To demodulate this Quantized Frequency Modulation a demodulator of the type described below is used. Fig. 3 is a block diagram which will be used in the following description.

The QFM signal is obtained from a standard communications receiver and is put through the four filters, but only one of four filters will pass a signal at any instant of time. The other three filters will pass only noise. The amplifier will amplify the signal to a maximum level if the signal is large enough to reach that level, otherwise it is amplified by the full gain of the amplifier. Each channel is full wave detected either positively or negatively, and the channels are added as shown in Fig. 3. The signals are then summed in the tapped delay line and differential amplifier.

The output of the differential amplifier is used to establish synchronization, which in turn gates the integrator to operate only during the time that the peak signal occurs.

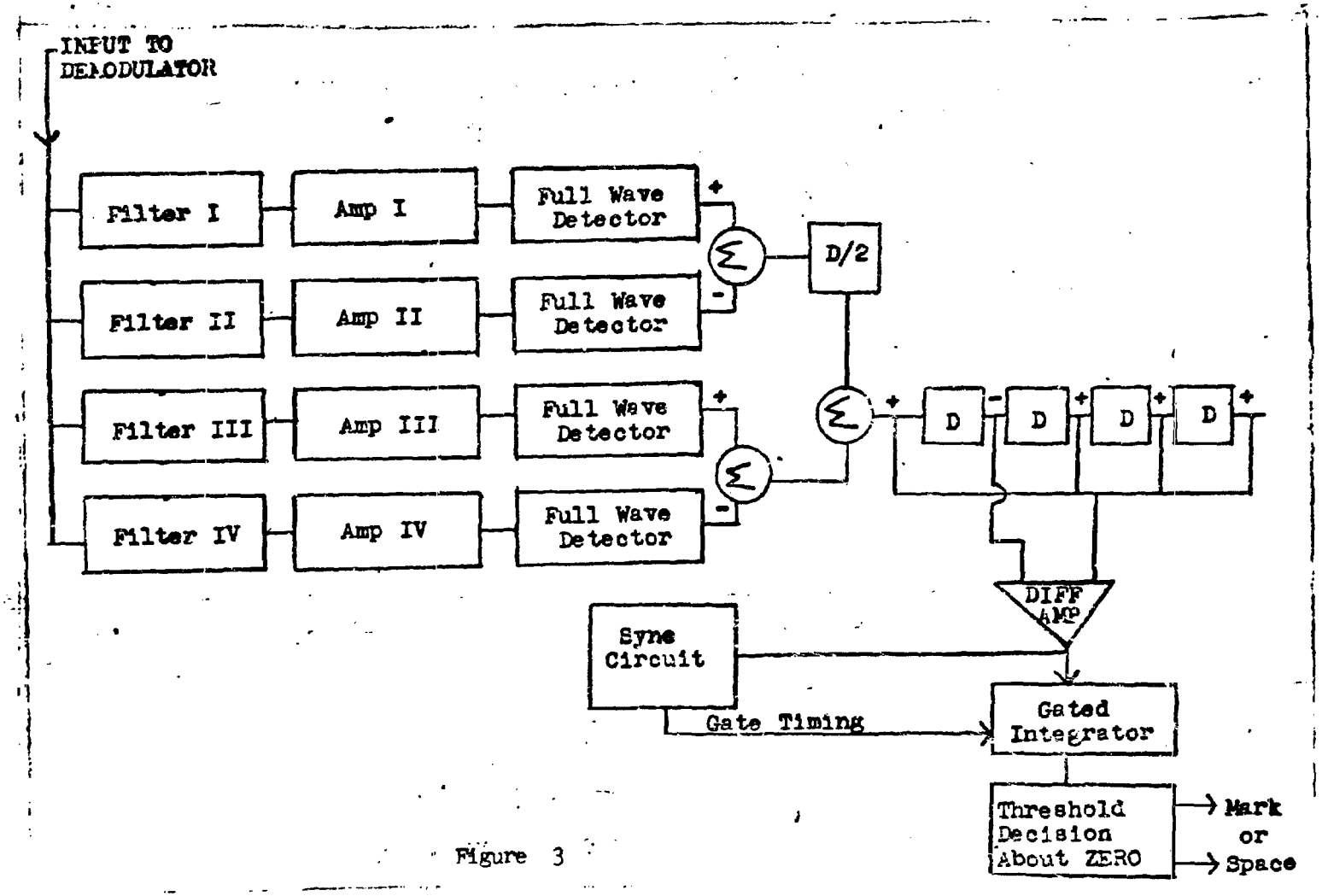
INPUT TO
DEMODULATOR
Filter I
Amp I
Full Wave Detector
Filter II
Amp II
Full Wave Detector
Filter III
Amp III
Full Wave Detector
Filter IV
Amp IV
Full Wave Detector
+
-
Σ
D/2
D
D
D
D
DIFF AMP
Sync Circuit
Gate Timing
Gated Integrator
Threshold Decision About ZERO
Mark
or
Space

Figure 3

The output of the gated integrator will be positive or negative depending on whether a "mark" or "space" code was transmitted. The output of the gated integrator is sampled just before the integrator capacitor is discharged. The sampling timing is also controlled by the synchronization circuit. The polarity of the integrator output will then determine whether the data is "mark" or "space" and will trigger the appropriate data flip-flop.

Since the decision is based solely on the polarity of integrator output the decision is made about a nearly zero threshold.

The operation of the system has been described. The principles of communication theory employed will be described where applicable in the following sections.

2.2 Short pulse and multi-frequency transmission.

The effect of multipath delay for pulses which are long compared to the delay time is shown in Fig. 4.

The effect of multipath delay for pulses which are short compared to the delay time is shown in Fig. 5.

It can be seen that the short pulse is more desirable, but of course this pulse requires more bandwidth, and contains less total energy.

Turning now to the selective fading effects of multipath propagation and directing our attention to Fig. 6, it may be noted that the multipath delay is different for different frequencies. So one possible approach to combatting selective fading could be by using more than one frequency in the transmission.

In this QFM scheme, the techniques and those to be described in Sections 2.3 and 2.4 are combined. In addition, in order to increase the total energy in a mark baud and space baud, ten pulses are transmitted for each baud. At the receiver the envelopes of these pulses are added coherently as described in the previous section.

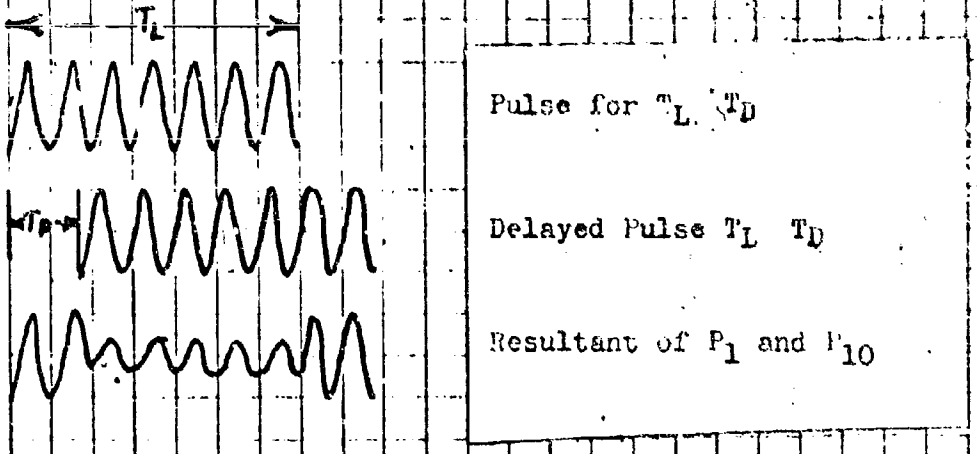

Pulse for T_L T_D

Delayed Pulse T_L T_D

Resultant of P_1 and P_{1D}

Figure 4

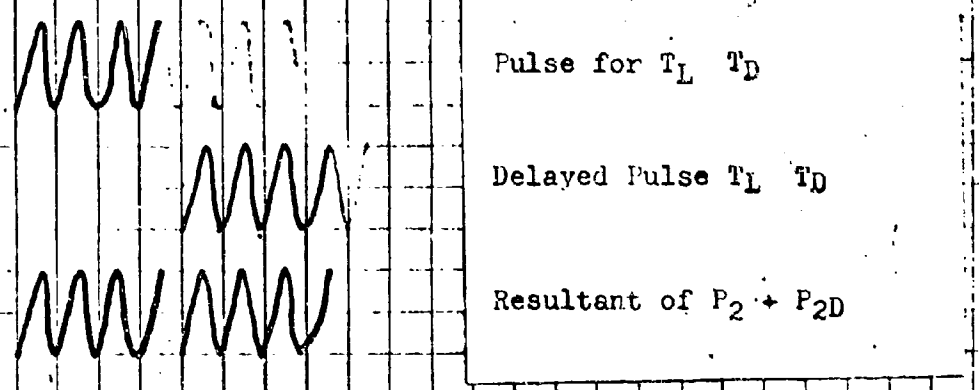

Pulse for T_L T_D

Delayed Pulse T_L T_D

Resultant of P_2 + P_{2D}

Figure 5

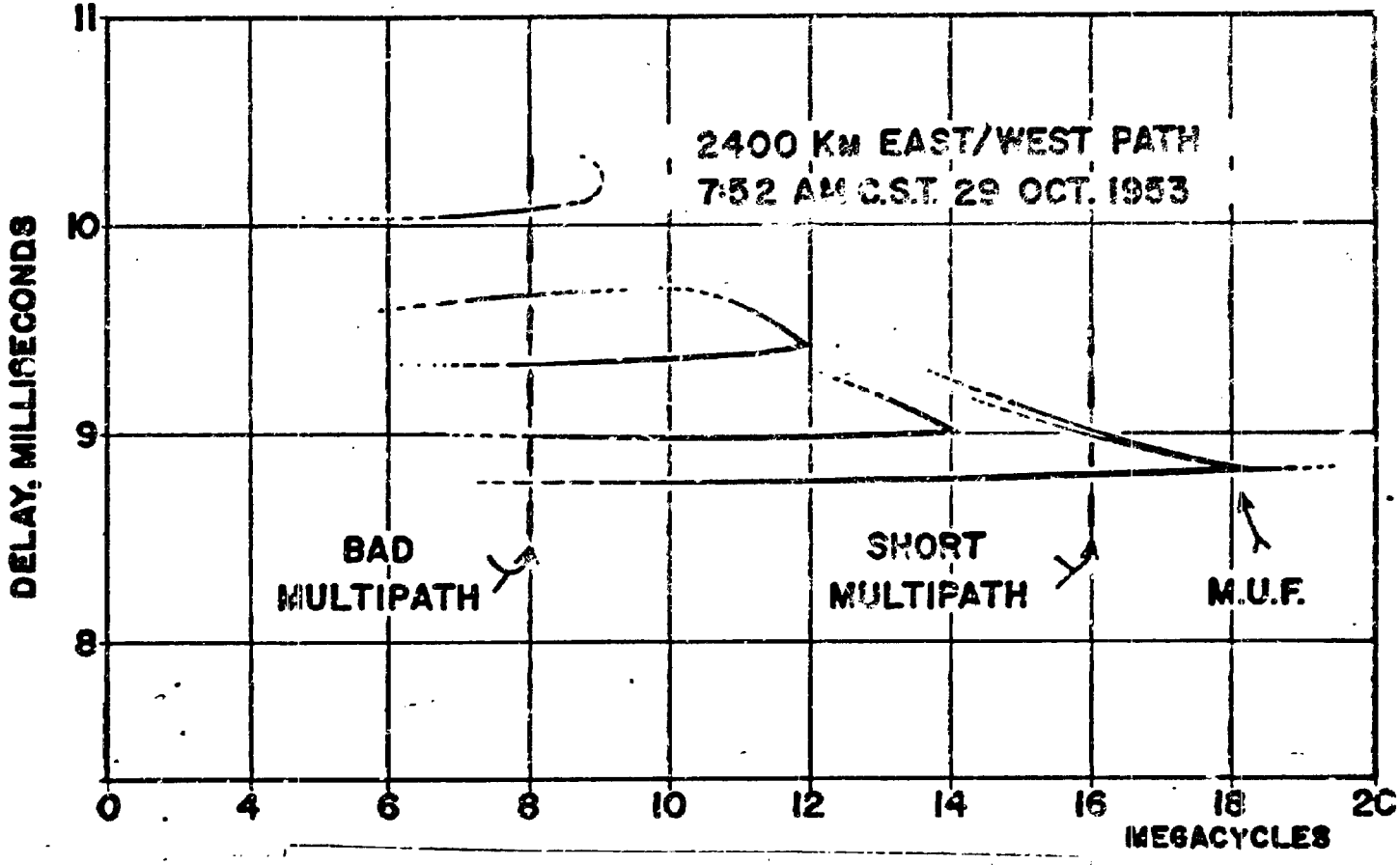

Sample of Variations of Time Delay with Frequency. From /17/.

Figure 6

2.3 Coded pulses and matched filter detection.

It has been shown /5/ that the optimum receiver to detect a signal in white Gaussian noise is one which calculates the likelihood ratio and then decides if a signal was present or not depending on whether the likelihood ratio exceeded a given threshold value or not respectively. The receiver which does this is a cross correlator, and essentially calculates the coefficient of linear correlation between the received signal and a copy of the transmitted signal. If this exceeds a specified value then the decision is made that a signal was present. Since this is a continuous process $\rho(\tau)$ is continuously being calculated as

$$\rho(\tau) = \lim_{T\to\infty} \frac{1}{T}\int_{-T/2}^{T/2} s_1(t)\, s_2(t-\tau)\, dt \qquad (1)$$

where $s_1(t)$ is the received signal and

$s_2(t)$ is the copy of the transmitted signal.

For application to the communications problem the decision to be made is, "Was the signal sent a mark or a space?". It has been shown, /1/ that the optimum decision process is one which calculates for both the mark and space by cross correlating the incoming signal with the "mark" signal as transmitted and the "space" signal as transmitted, and then decides which is larger.

Thus $$\rho_{space}(\tau) = \lim_{T\to\infty} \frac{1}{T}\int_{-T/2}^{T/2} s(t)\, s_{space}(t-\tau)\, dt \qquad (2)$$

and $\rho_{mark}(\tau) = \lim_{T\to\infty} \frac{1}{T} \int_{-T/2}^{T/2} s(t)\, s_{mark}(t-\tau)\, dt$ (3)

where $s_{space}(t)$ is the signal representing "Space" and $s_{mark}(t)$ is the signal representing "Mark".

It has also been shown /1/ that the probability of making a wrong decision is least when mark space and the decision threshold is zero. The cross correlation of the "mark" signal as transmitted with a "space" signal as transmitted for this case would be -1.

One means of implementing a cross correlation detector is by means of a filter. The output of a filter for a given input signal is the convolution of the signal with the impulse response of the filter.

$$y(t) = \int_{-\infty}^{\infty} x(\tau)\, h(t-\tau)\, d\tau \qquad (4)$$

or

$$y(\tau) = \int_{-\infty}^{\infty} x(t)\, h(\tau-t)\, dt \qquad (5)$$

if the impulse response of the filter h(t) is the time reverse of the input signal, X(+t), then the output is the convolution of X(t) with X(-t). Substituting in equation (5) above

$$y(\tau) = \int_{-\infty}^{\infty} x(t)\, x(\tau-(-t))\, dt \qquad (6)$$

$$y(\tau) = \int_{-\infty}^{\infty} x(t)\, x(\tau+t)\, dt \qquad (7)$$

$$y(\tau) = \int_{-\infty}^{\infty} x(t)\, x(t+\tau)\, dt \qquad (8)$$

Since $\rho(\tau)$ as shown in equation (1) is an even function for periodic signals

$$\rho(\tau) = \rho(-\tau) \qquad (9)$$

from (1)

$$\rho(\tau) = \rho(-\tau) = \lim_{T\to\infty} \frac{1}{T} \int_{-T/2}^{T/2} x(t)\, x(t+\tau)\, dt \qquad (10)$$

In any physical implementation, integration starts at some time t_o and is carried out for some finite time interval. Hence

$$\rho(\tau) \doteq y(\tau)$$

for any physically realizable system.

In terms of probability, the question, "Given that a signal was sent, what is the probility that it was a "mark" and what is the probability that it was a "space" ?" must be answered. Since each is equally likely, the a priori probability of each is one-half.

The a posteriori probability that a mark (for instance) was sent is, from /1/

$$P(s_{mark}(t)/f(t)) = \frac{P[f(t)/s_{mark}(t)] \cdot P[s_{mark}(t)]}{P[f(t)/s_{mark}(t)]P[s_{mark}(t)] + P[f(t)/s_{space}(t)]\, P[s_{space}(t)]}.$$

It has been shown /1/ that for mark and space equally likely the decision reduces to:

"Decide "mark" if

$$\int_0^T f(t)\, s_{mark}(t)\, dt - \int_0^T f(t)\, s_{space}(t)\, dt \qquad (12)$$

is greater than zero (positive). Decide "space" if (12) above is less than zero (negative).

If a truly matched filter or correlation detector could be built the error rate has been shown to be

$$P_E = \int_0^\infty \frac{1}{2\pi\sqrt{2EN_0}} \exp\left[-\frac{(x+E)^2}{4EN_0}\right] dx. \qquad (13)$$

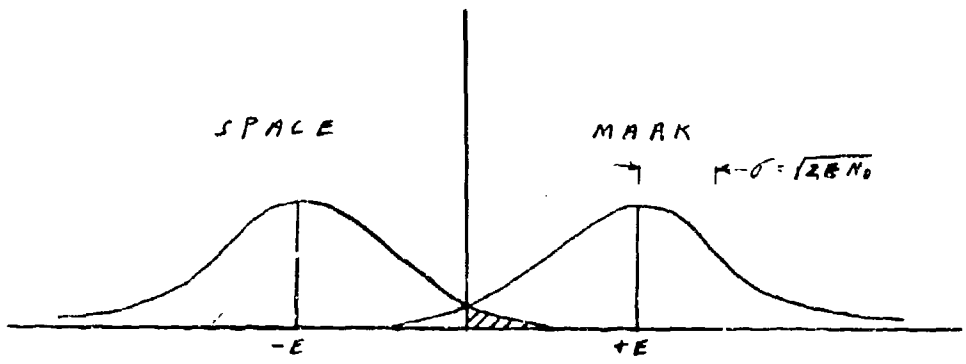

Figure 7

2.4 Tapped delay line approximization to a matched filter.

Turin /6/ proposed three methods of implementing a matched filter. One of these was the tapped delay line. However, he pointed out that there are physical limitations to this approach. The filter which is truly matched is matched continuously from beginning to end of the signal when $\tau = 0$. Fig. 8 shows an example of a signal and the impulse response of a filter matched to it.

signal

h(t) for filter matched to signal

Figure 8.

A signal which might be put into a tapped delay line and its corresponding matched filter is shown in Fig. 9.

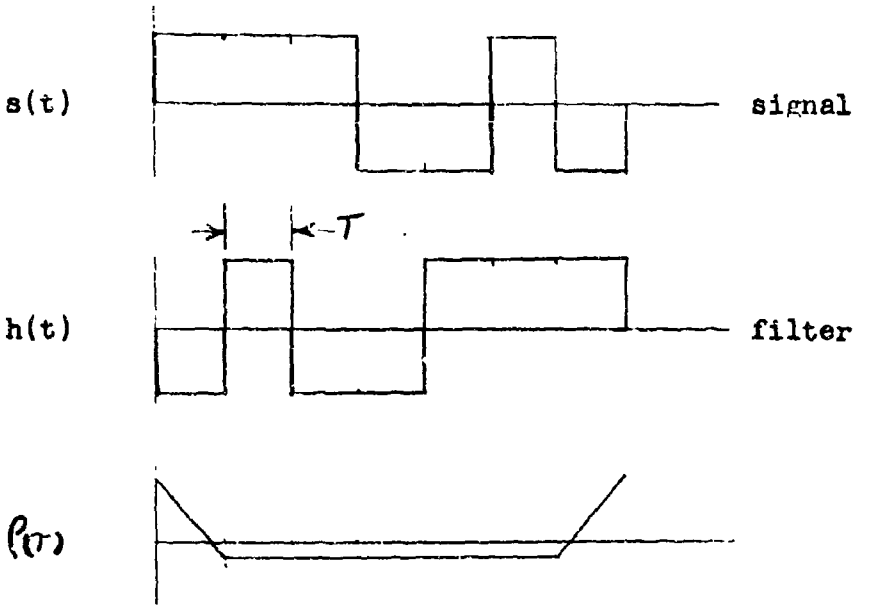

Figure 9

This particular signal pattern chosen is one of the well known "Barker codes" /7,8/. It was chosen to illustrate a desirable property which is possessed by some binary codes, namely that of a "good" autocorrelation function. Notice that the interval between peaks is flat.

However if instead of a truly matched filter a tapped delay line is used, the output of the filter is still the correlation of the input signal with the impulse response of the filter, but the taps are not as "broad" as the pulse length. Instead the taps could be represented as delta functions weighted by the proper sign as shown in Fig. 10.

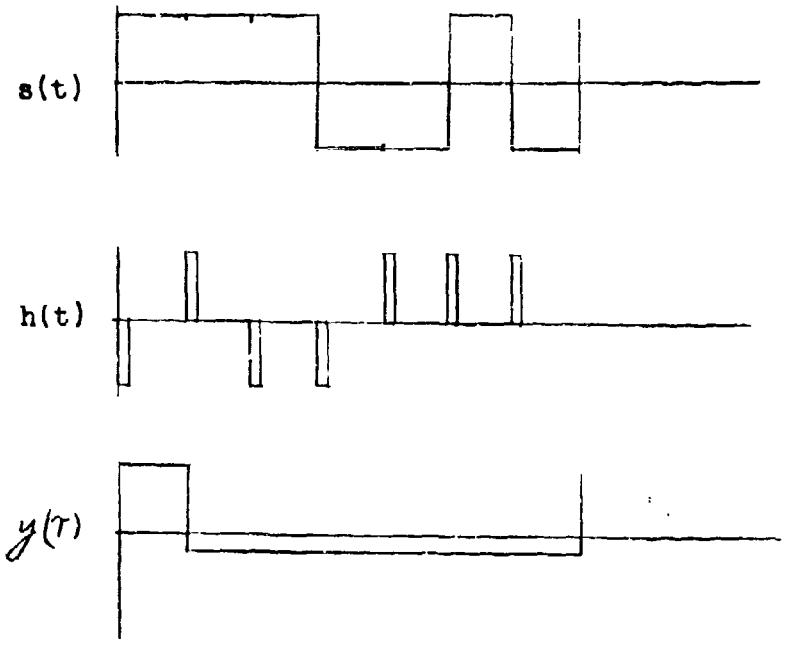

Figure 10

Notice that the output $y(\tau)$ at $\tau = 0$ has the shape of an individual signal of width T instead of the triangle. The delay line it is seen, linearly adds the voltages at each tap, and is not truly "matched" to the signal. The next section will deal with the analysis of the system, and will establish a mathematical model to predict theoretical performance maxima.

3. Analysis of Demodulator.

3.1 Mathematical model of demodulator.

In order to analyze the performance of the system and to be able to predict error rates for various signal to noise power ratio inputs a mathematical model was devised. Models have been established and performance analysis done for several of the well known binary communications systems. /9,10,11/ However most of these analyses assume a signal to noise ratio of 3db or more. This paper deals with lower signal to noise power ratios and consequently the approximation used in them are not valid for this study. The signal to noise power ratios in and out of an envelope detector have been described completely by Rice. /12/ Techniques in the application of his results may be found in other publications as well. /13, 14/

The exact expression for the density function of the output of an envelope detector includes a modified Bessel function. At this point the high speed digital computer was used to obtain the signal voltage and noise power for different signal to noise ratios. This system is essentially linear from input to the full wave rectifier of each channel, and subsequent to that. Hence if the non-linearity of the full wave rectifier could be analyzed and modeled then the entire system could be modeled. The amplifier prior to detection will be assumed linear, and section two demonstrated that the tapped delay output was the linear alge-

braic sum of the signal in the filter at every instant of time. Hence the signal to noise power ratio at the input to the full wave detector will be taken as a reference. Signal to noise power ratios at the input to the demodulator can then be expressed in terms of the reference. In making the transition from full wave rectifier input to demodulator input it will be assumed that the noise figure for the AGC amplifier is zero.

Another assumption in the model is that the signal pulse is a square pulse. This is done in order to simplify the analysis of the model. However in order to use the model to relate predicted error rates to actual error rates measured a conversion factor is used. Appendix IV shows in detail how this conversion factor is calculated. Once the relationship is made the relative positions of the predicted curve to the actual measured error rate curve is established. The error rate versus signal to noise ratio per pulse at the input to the detector can be used as a reference, and error rates for signal to noise ratio at any point before the detector can then be obtained. This relationship may be seen by comparing the graphs of Fig. 19 and Fig. 20.

The model is considered to have four separate channels. Each channel has an ideal filter 580 cycles wide centered at 680, 1260, 1940, and 2620 cps. The signals of each channel are envelope detected and added together as shown in Fig. 3. The output of the tapped delay line is inte-

grated for one half the pulse period during the time interval that the summed pulse is highest. A decision is then made at the end of integration time on the basis of the polarity of the integrator output. "Mark" if the integrator output is positive and "Space" if the integrator output is negative.

The probability of error is the probability that the integrator output will be negative (or positive) when a "Mark" (or "Space") signal was transmitted.

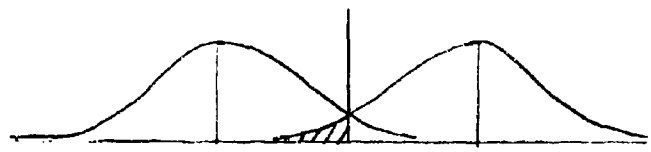

Figure 11

From Fig. 11 it may be seen that the probability of error is:

$$P_e = \int_{-\infty}^{0} \frac{1}{\sqrt{2\pi}\,\sigma_N} \; EXP - \left[\frac{(x-M)^2}{2\sigma_N^2} \right] dx$$

In order to take advantage of the tabulations of the area under the normal curve /15/ this is put into the form

$$P_e = \frac{1}{2} \left[1 - Erf\ V \right]$$

where Erf V = $\frac{1}{\sqrt{2\pi}} \int_{-V}^{V} EXP - \left[\frac{x^2}{2} \right] dx$

3.2 Analysis of model.

It has been shown by Rice /11/ that if an envelope detector has as its input bandlimited white Gaussian noise, the probability density function for the output is the Rayleigh distribution. Specifically for an input or bandlimited white Gaussian noise of power spectral density N_o watts per cycle per second, the output of an envelope detector has as its probability density function the Rayleigh distribution,

$$p(y) = \frac{1}{N^2} y e^{-y^2/2N^2}$$

where $N^2 = N_o B$.

The power spectral density and probability density function is as shown in Fig. 12. As a signal is added to the noise input, the density function shifts to the right as shown in Fig. 13 and Fig. 14.

The probability density function for the output is now a function of the signal power and the noise power. Specifically from /14/

$$p(y) = \frac{y}{\sigma_N^2} e^{-s^2} e^{-y^2/2\sigma_N^2} I_o\left(y s \frac{\sqrt{2}}{\sigma_N}\right)$$

where $I_o(x)$ is the Modified Bessel function of the first kind and zero order for the argument x, and s^2 is the signal to noise power ratio for a continuous carrier. Most treatments of envelope detectors will make a closed

form approximation to $I_o(x)$ for large or small signal to noise ratios, because the density function becomes essentially normal for large signal to noise ratios, and $I_o(x)$ can be closely approximated by $e^{\frac{x^2}{4}}$ for $x \ll 1$. However for this study these approximations were crudest in the region of main interest. The modified Bessel function $I_o(x)$ may be expressed as the sum of an infinite series, namely

$$I_o(x) = \sum_{n=0}^{\infty} \frac{x^{2n}}{2^{2n}(n!)^2} .$$

Appendix I shows the infinite series solution to obtaining the mean, and variance of the resulting probability density function.

Appendix II is the computer programs used to calculate the mean and variance of the distribution resulting from different signal to noise power ratios at the input to the envelope detector. The program also includes some other calculations used to obtain the probability of error which would have been quite laborious if done by hand. Also included in Appendix II is a sample of the program outputs.

Fig. 16 illustrates an example of the probability density functions for all four channels at one instant of time, and how they are combined.

Although the distribution of the sum of the four

channels is not truly normal, it is nearly so. After summing ten of these nearly normal distributions, by the central limit theorem, the resulting distribution will be very close indeed to being a normal distribution.

This signal is then integrated for an int rval of 2 milliseconds. Appendix III describes the treatment of integrating a signal plus noise. For a continuous carrier pulse this amounts to reducing the signal to noise power ratio. The result is manifest on the distribution function as a change in the ratio of the D. C. signal level to the standard deviation of the distribution, and the probability of error is reduced accordingly. Probability of error is now

$$P_E = \tfrac{1}{2} \quad 1\text{-Erf } Q$$

where $Q = \dfrac{10(\mathcal{M}_1 - \mathcal{M}_2)\ (1.2)}{\sqrt{10(\sigma_1^2 + 3\sigma_2^2)}}$

$\mathcal{M}_1$ is the mean of distribution of the output voltage of the channel containing the signal during one pulse duration. σ_1^2 is the variance of the distribution of the output of the channel containing the signal during one pulse duration, or fluctuation noise power.

$\mathcal{M}_2$ is the mean of the Rayleigh distribution resulting from envelope detection of white Gaussian noise. σ_2^2 is the variance of the Rayleigh distribution or fluctuation noise power of the output of envelope detection of white Gaussian noise.

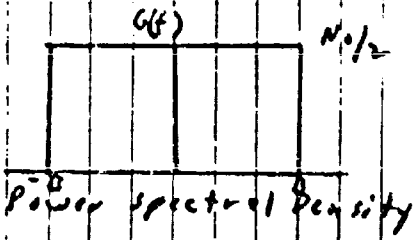

Power spectral Density

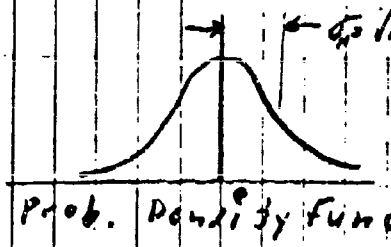

Prob. Density function

White Gaussian Noise

Fig 12

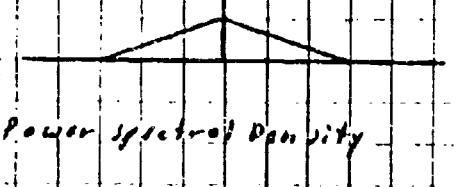

Power spectral Density

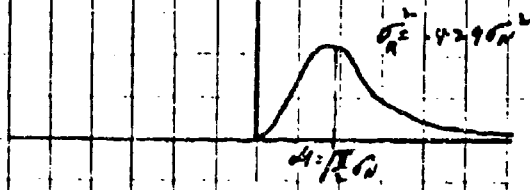

Probability Density Function

Output of Envelope Detector for a White Gaussian Noise Input

Figure 13

Power spectral Density

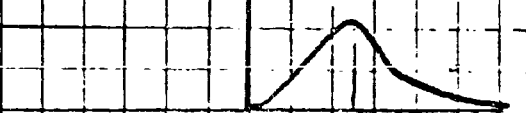

Probability Density function.

OUTput of Envelope Detector for a Signal Plus Noise Input.

Figure 14

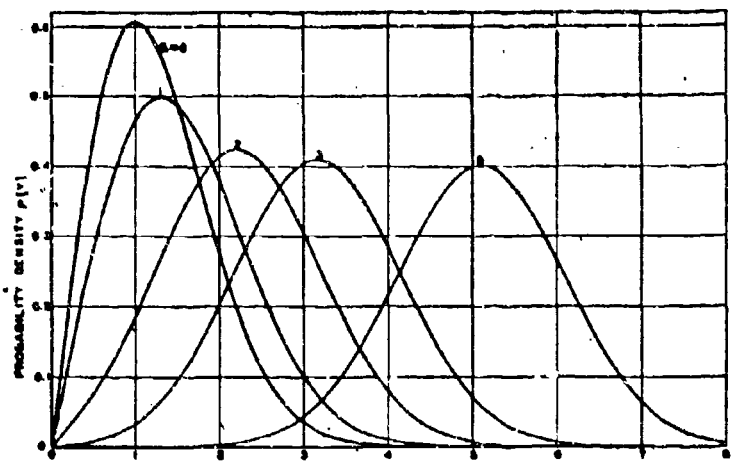

Probability Density Function for the Output of an Envelope Detector for Increasing Signal to Noise Ratio. From /11/.

Figure 15

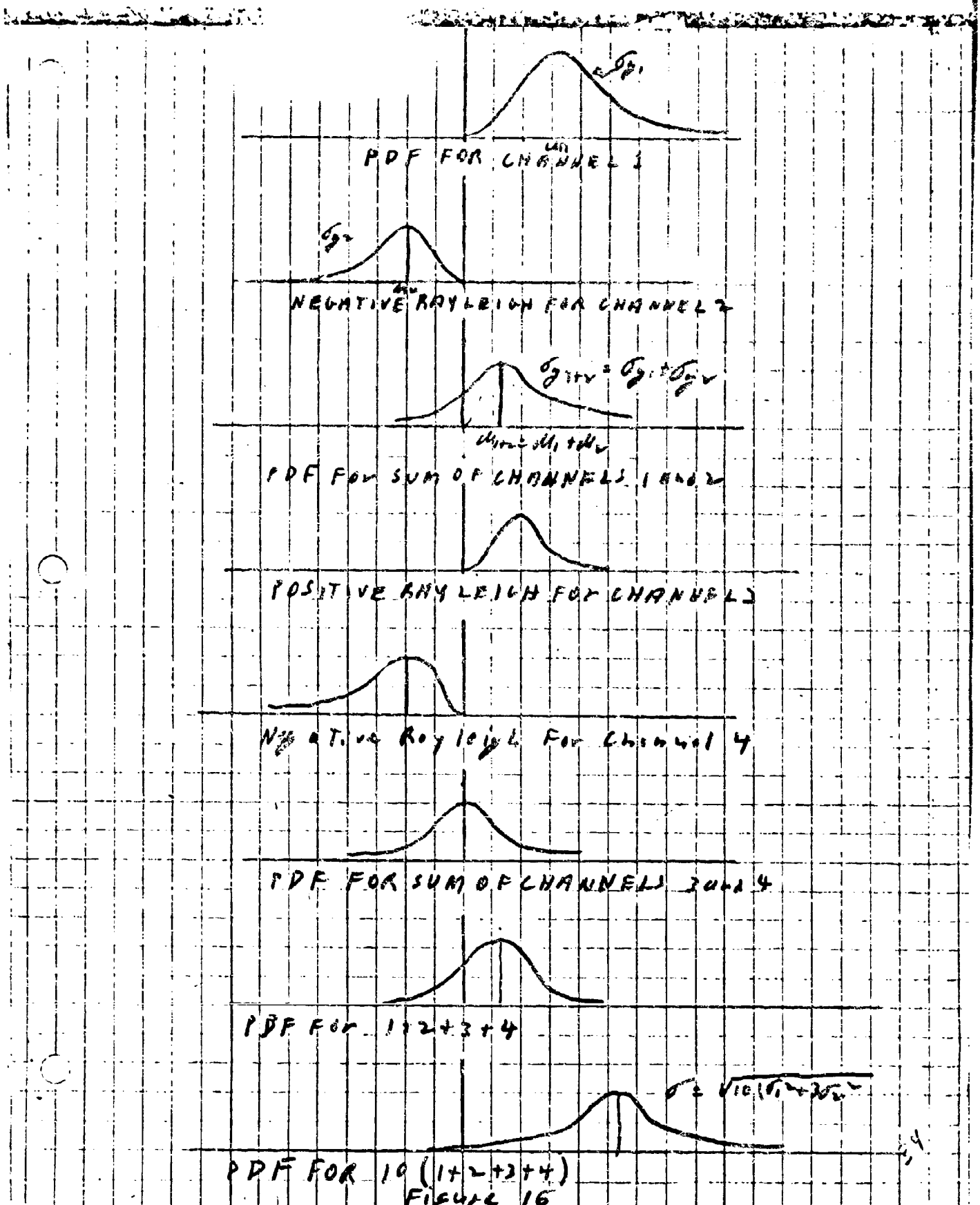
PDF FOR CHANNEL 1
NEGATIVE RAYLEIGH FOR CHANNEL 2
PDF FOR SUM OF CHANNELS 1 AND 2
POSITIVE RAYLEIGH FOR CHANNEL 3
NEGATIVE RAYLEIGH FOR CHANNEL 4
PDF FOR SUM OF CHANNELS 3 AND 4
PDF FOR 1+2+3+4
PDF FOR 10 (1+2+3+4)

Figure 16

The standard deviation of the Gaussian noise distribution was taken as one, and thus the noise power σ_N^2 was one. Then the signal to noise power ratio is just the signal power. A Control Data Corporation 1604 computer was used to calculate Q and the probability of error obtained from tables /15/. The probability of error for various signal to noise power ratios was obtained and plotted. Curve V of Fig. 19 is the curve obtained.

Laboratory measurements were made to compare actual error rates with those predicted. A description of the apparatus and techniques used and the results obtained is contained in the next two sections.

4. Laboratory Tests of Demodulator.

A laboratory test of the demodulator was desired to compare actual performance with the theoretical predictions. In order to do this it was necessary to devise some means of detecting and counting errors and counting decisions made. Appendix V is a description of the error detector which was built up from Engineered Electronics Company digital building blocks. Fig. 17 is a block diagram of the laboratory equipment layout.

The automatic gain control circuits of the amplifier were set for minimum gain, and the linear range of the amplifier was determined. Fig. 18 is an example of the linear range of the amplifier.

A few tests showed that the error rate was quite good for good signal to noise ratios but seemed to have a signal to noise ratio threshold below which the demodulator lost synchronization. Actual errors as a result of wrong decisions were still quite low.

Investigation of the synchronization circuits revealed that for the signal to noise ratio at which the demodulator lost synchronization, there was still available a reasonably "clean" signal pulse coming from the differential amplifier. However the voltage level of the signal was not of sufficient amplitude to be sensed by the part of the synchronization circuit which decided if a signal (either "mark" or "space") was present. A two stage amplifier was then inserted between the differential amplifier

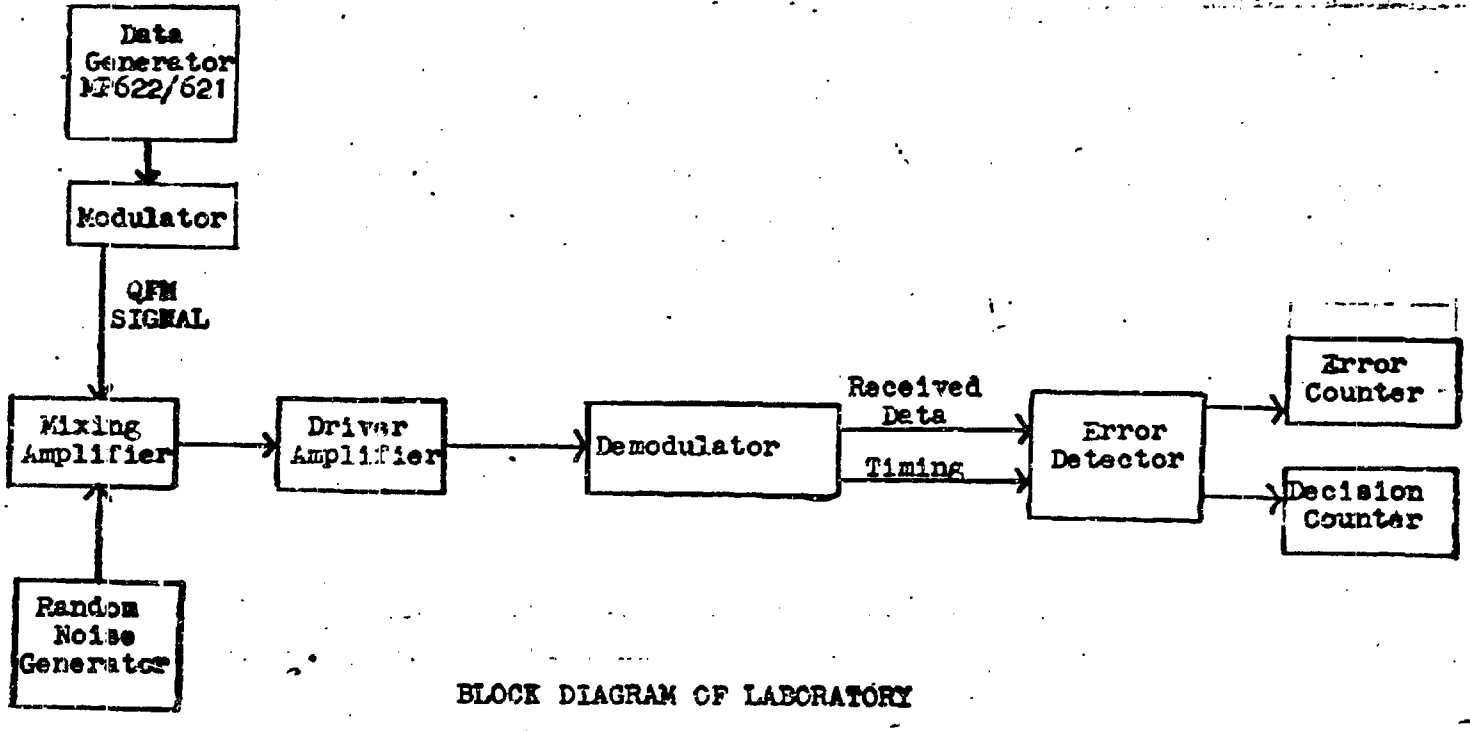

BLOCK DIAGRAM OF LABORATORY TEST SETUP

Figure 17

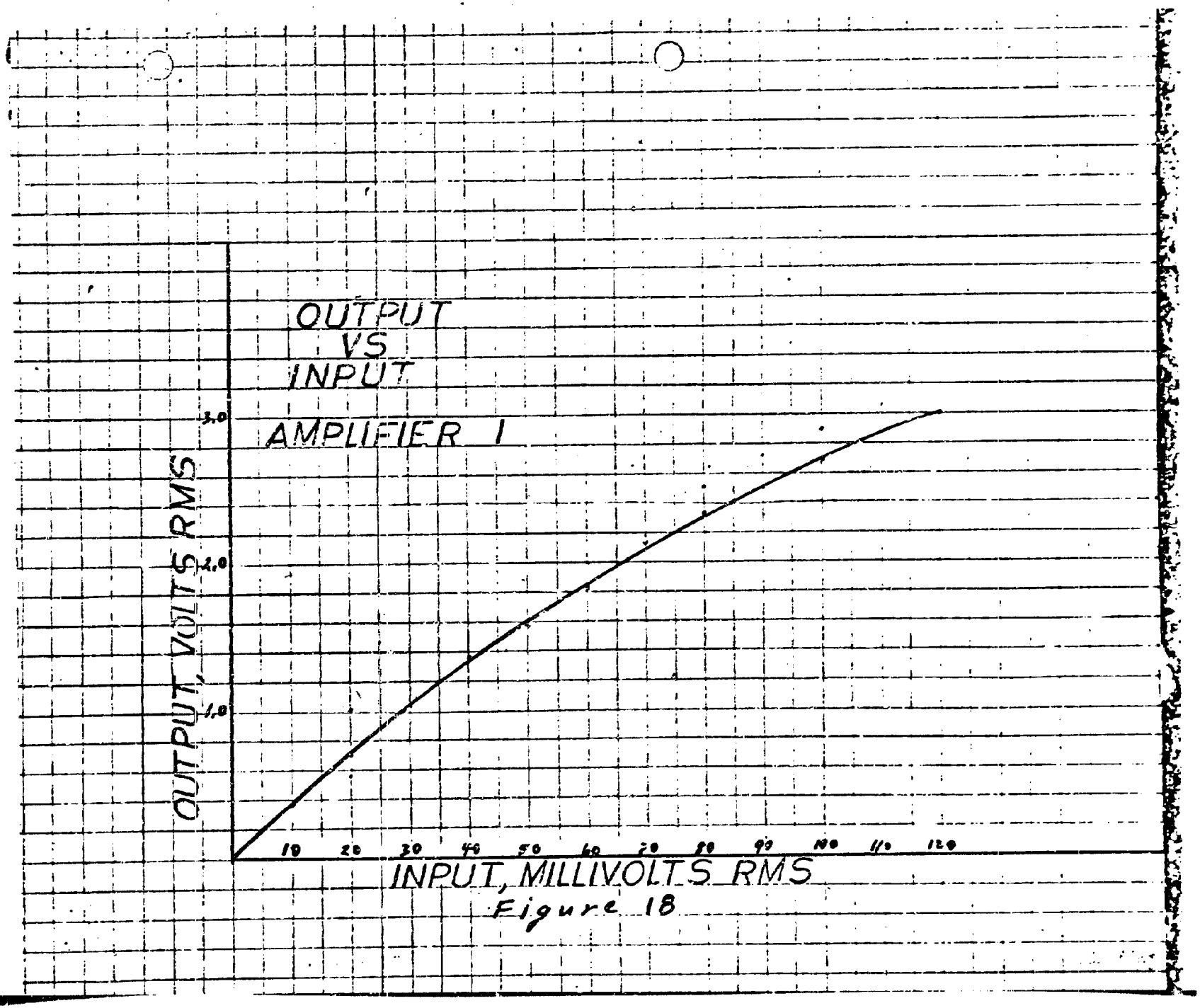
OUTPUT
VS
INPUT
AMPLIFIER 1
OUTPUT, VOLTS RMS
3.0
2.0
1.0
10
20
30
40
50
60
70
80
90
100
110
120
INPUT, MILLIVOLTS RMS
Figure 18

and the "signal sensing" portion of the synchronization circuit. Curve II of Fig. 19 is the curve of error rates measured for this configuration.

Visicorder recordings of the outputs of the gated integrator and data output showed that additional improvement could be obtained. The time constant of the operational amplifier integrator was reduced. The error rates obtained for this configuration is shown as curve III of Fig. 19.

Visicorder recordings show that the sensing threshold was considerably above zero. The input resistance to the sensing transistors was reduced to allow the required switching current to be reached at a lower threshold voltage. This was the final configuration tested, and the error rates for it are shown as curve IV of Fig. 19.

In Fig. 19 the measured signal to noise ratio was corrected to fit the model as described in Appendix IV. Fig. 19 is the same data referring the model signal to noise ratios to the measured signal to noise ratio per bit.

As discussed in section 3, the data in Fig. 19 and 20 are for the signal to noise ratio at the input to the full wave rectifier as a reference, in order to refer the error rate to the signal to noise ratio per bit at the input to the filters the following correction is required.

Each filter bandwidth is 580 cps. The total noise bandwidth at the input is 3 kc — 400 cps = 2500 cps. There is then $\frac{2600}{580}$ or 4.5 times as much noise per bit at the input as in each channel. Signal to noise ratio must then be reduced by 6.53db. Fig. 21 shows this.

Any measurements made in the future on this system will probably be done by a true reading RMS voltmeter as was done in our experiments. Figs. 19, 20, and 21 are on a signal to noise power per bit basis. Since the signal was a mark--space--mark--space, etc., the average signal power was just one-half of the power per bit. Average signal to noise power ratio is then 3db less for each rate than for Fig. 21. This is shown in Fig. 22, and is the error rate for the signal to noise ratio which would be measured at the input to the demodulator.

Fig. 23 is a group of pictures showing the QFM signal, the differential amplifier, output for two signal to noise ratios and configurations.

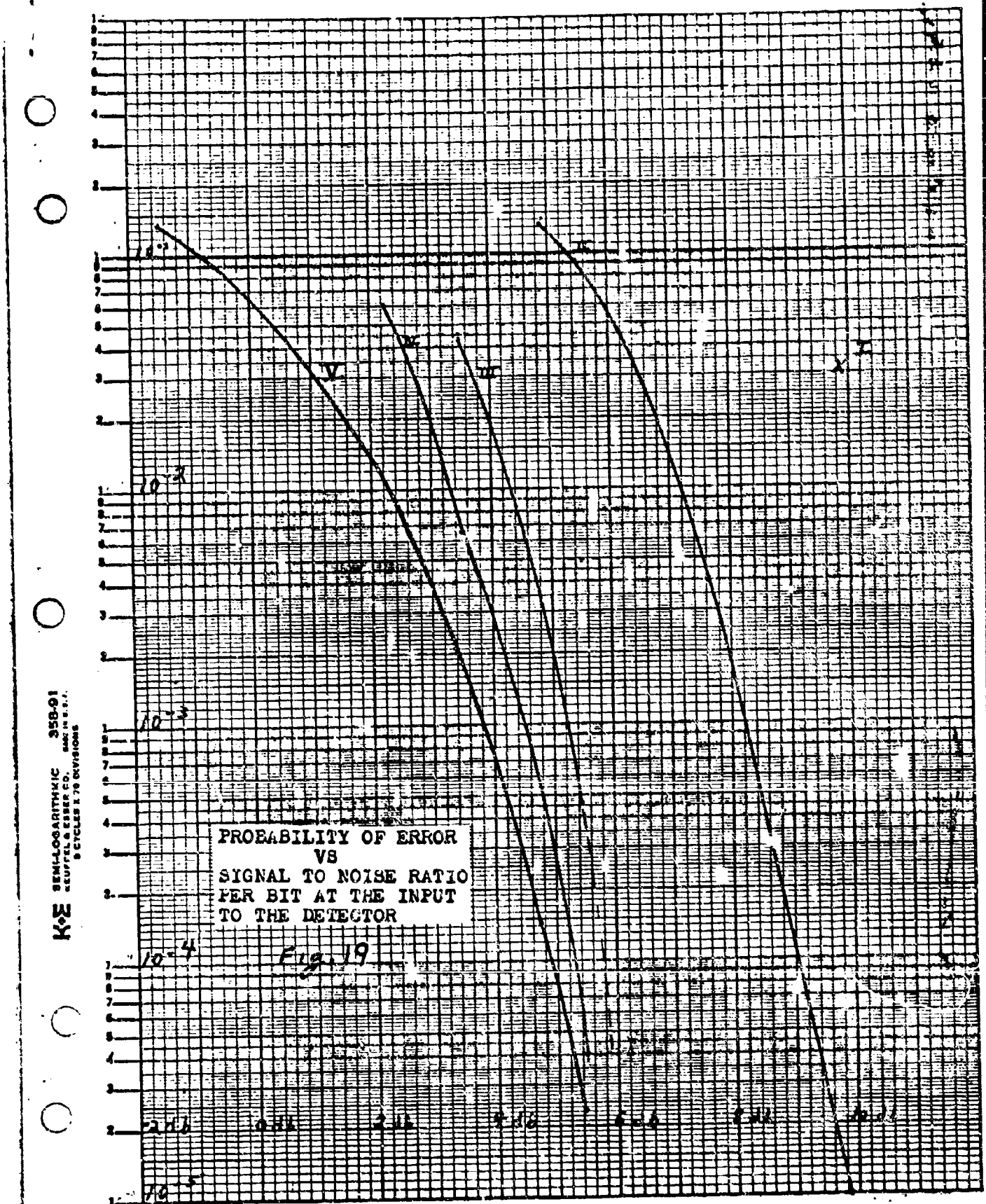
PROBABILITY OF ERROR
VS
SIGNAL TO NOISE RATIO
PER BIT AT THE INPUT
TO THE DETECTOR
Fig. 19
10⁻²
10⁻³
10⁻⁴
10⁻⁵
K&E
SEMI-LOGARITHMIC 358-91

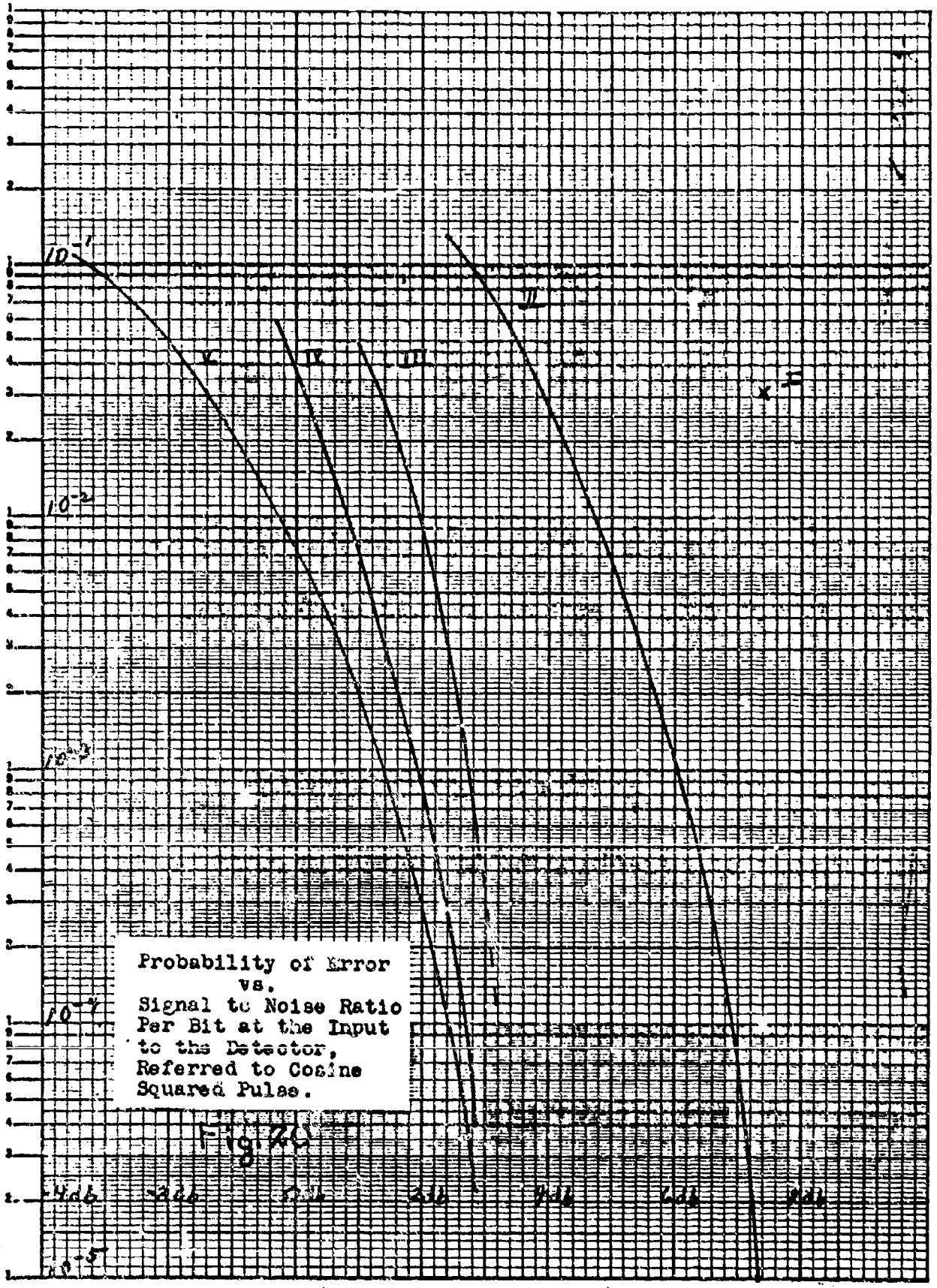

Probability of Error
vs.
Signal to Noise Ratio
Per Bit at the Input
to the Detector,
Referred to Cosine
Squared Pulse.

Fig. 20

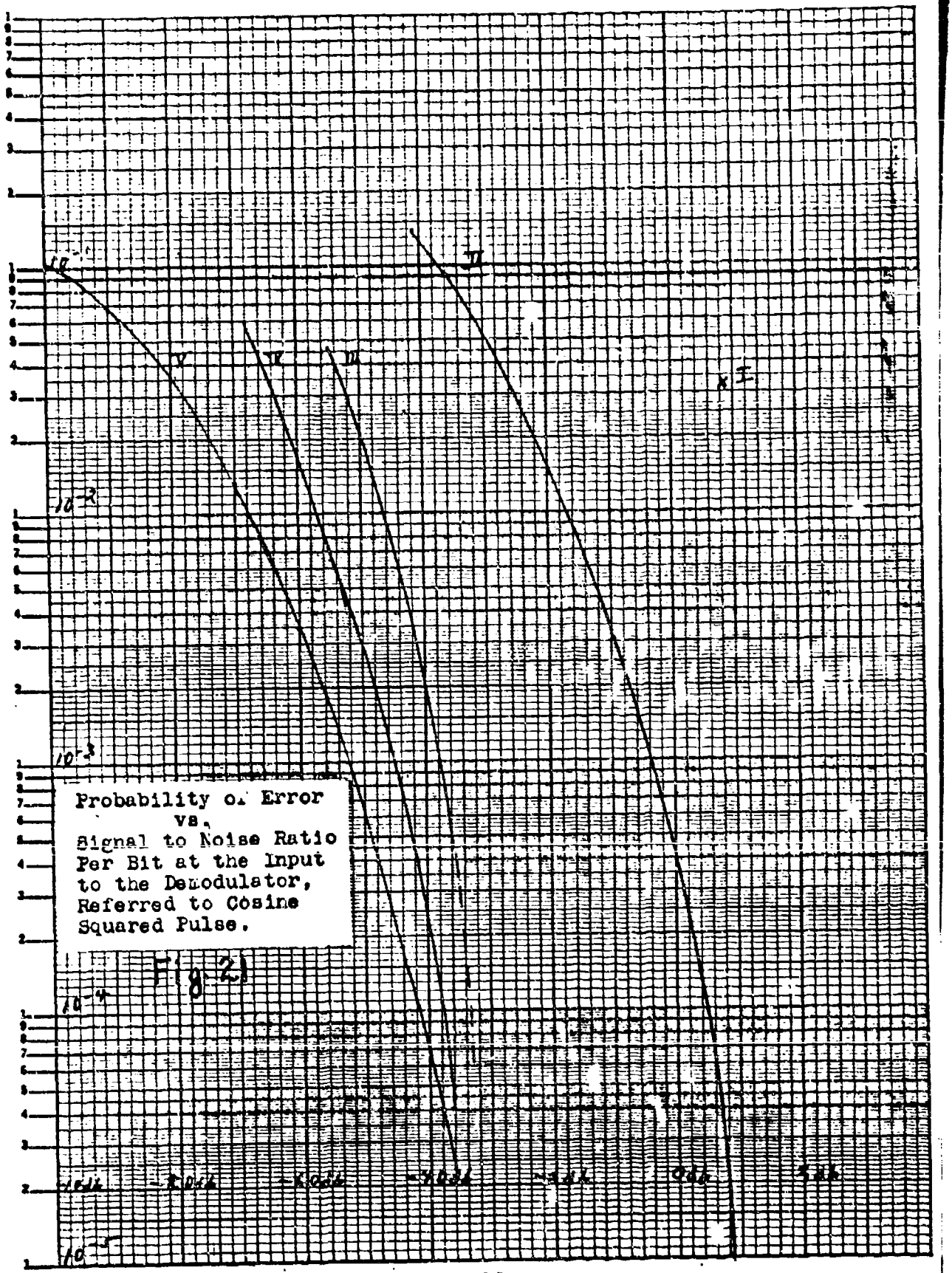

Probability of Error vs. Signal to Noise Ratio Per Bit at the Input to the Demodulator, Referred to Cosine Squared Pulse.

Fig 2)

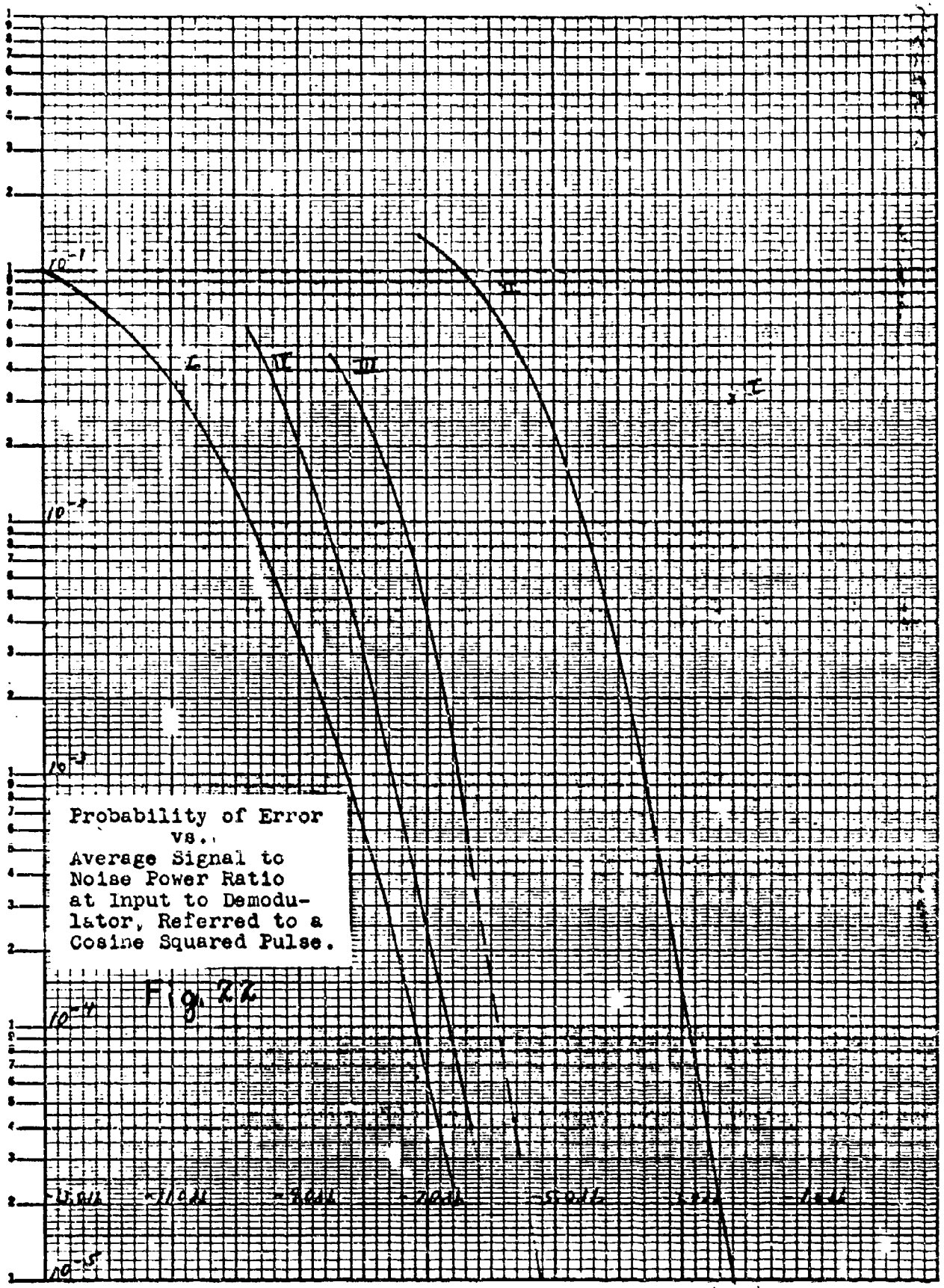

Probability of Error vs. Average Signal to Noise Power Ratio at Input to Demodulator, Referred to a Cosine Squared Pulse.

Fig. 22

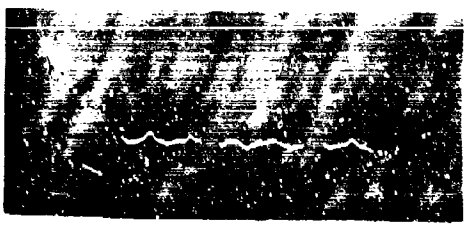

5v/cm PRK signal (no noise)
.5v/cm differential amplifier output

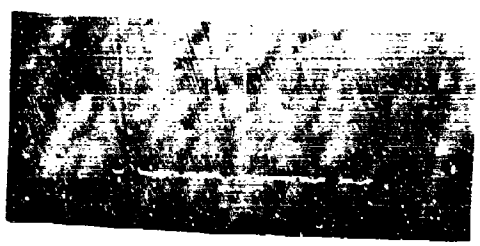

10v/cm PRK signal + noise
S/N (per bit) = 243db (Ref COS^2)
1v/cm output of differential amplifier
P_E (II) = .16

5v/cm gated integrator output
1v/cm output of differential amplifier
P_E = .16 (II)

.5v/cm differential amplifier output
S/N (per bit) = .3db (Ref COS^2)
5v/cm gated integrator output
PE (IV) = .059

5v/cm gated integrator output
5v/cm data output
P_E (IV) = .059

Figure 23

5. Conclusions.

A close analysis of a system to obtain a theoretical optimum performance level provides a useful standard to which actual performance may be compared. Such an analysis may show the possible improvement to be gained by alterations in various sections of a system. Such was the case for the QFM system studied. Curve V is the theoretical optimum performance criteria for this system, and I to IV are performance levels for various configuations of the system. It appears that additional improvements in system performance are still possible. However these curves cannot show the limitations of the synchronization circuit. Perfect synchronization and zero threshold are assumed.

In any physically realizable system synchronization is not perfect and the threshold is some small value above and below zero.

BIBLIOGRAPHY

1. E. J. Baghdady, Lectures on Communication System Theory, McGraw-Hill Book Co. Inc., New York, 1961.

2. J. L. Eckessley, Multiple Signals in Short Wave Transmission, Proc. I.R.E., Vol. 16, pp. 106-122, Jan., 1930.

3. J. P. Costas, Synchronous Communications, Proc. I.R.E., Vol. 44, pp. 1713-1718, Dec. 1956.

4. R. Price and P. E. Green, A Communication Technique for Multipath Channels, Proc. I.R.E., Vol. 46, No. 3, pp. 555-570, March, 1958.

5. W. W. Peterson, T. G. Birdsall, and W. C. Fox, The Theory of Signal Detectability, I.R.E. Trans. PGIT-4, I.R.E., Sept., 1954.

6. G. L. Turin, An Introduction to Matched Filters, I.R.E. Trans Vol. IT, pp. 311-329, June, 1960.

7. R. H. Barker, Group Synchronization of Binary Digital Systems in Communication Theory. W. Jackson, Ed., Academic Press, New York, New York, 1953.

8. B. Elspas, A Radar System based on Statistical Estimation and Resolution Considerations, Technical Report N. 361-11, Amplified Electronics Laboratory, Stanford, California, August 1, 1955.

9. A. B. Glenn, Performance Analysis of a Dat Link System, I.R.E. Trans., Vol. CS-7, No. 2, pp. 14-24, May 1959.

10. A B. Glenn, Comparison of PSK vs. FSK and FSK-AM vs FSK-AM Binary Coded Transmission Systems, I.R.E. Trans., Vol. CS-8, No. 3, pp. 87-100, June, 1960.

11. S. O. Rice, Mathematical Analysis of Radar Noise, Bell System Technical Journal, Vol. 23, pp. 282-332, July, 1944, and Vol. 24, pp. 46-156, Jan., 1945.

12. G. F. Montgomery, A Comparison of Amplitude and Angle Modulation for Narrow Band Communication of Binary Coded Messages in Fluctuation Noise, Proc. I.R.E., Vol. 42, No. 2., pp. 447-454, Feb. 1954.

13. W. R. Bennett, Methods of Solving Noise Problems, Proc. I.R.E., Vol. 44, No. 5, pp. 609-638, May, 1956.

14. M. Schwartz, Information Transmission, Modulation, and Noise, McGraw-Hill Book Co., Inc., New York, 1959.

15. National Bureau of Standards, Tables of Probability Functions, Vol. II, 1942.

16. N. Abramson and J. Farison, On Statistical Communication Theory, Tech. Report No. 2005-1, Standford Electronics Laboratory, August, 1962.

17. G. L. Evans, "State-of-the-Art Evaluation Quantized Frequency Modulation", Final Report, USAF 480L System, Communications Div., Hughes Aircraft Co., Jan., 1960.

APPENDIX I

Infinite Series Solution to Mean and Variance of the Probability Density Function for the Output of an Envelope Detector for Various Signal to Noise Power Ratios

From /11/ the probability density function for the output of an envelope detector is

$$p(x) = \frac{e^{-S^2} x\, e^{-\frac{x^2}{2\sigma_N^2}}}{\sigma_N^2} I_0\left(xS\frac{\sqrt{2}}{\sigma_N}\right)$$

where

S^2 is the signal to noise power ratio at the input to the envelope detector,

N^2 is the noise power at the input and

$I_0(Y)$ is the modified Bessel function of the first kind and zeroth order of the argument Y .

$I_0(Y)$ can be expressed as the sum of an infinite series

$$I_0(Y) = \sum_{n=0}^{\infty} \frac{Y^{2n}}{2^{2n}(n!)^2}$$

The mean of this distribution is

$$M = \int_{-\infty}^{\infty} \left[\frac{x^2 e^{-S^2} e^{-\frac{x^2}{2\sigma_N^2}}}{\sigma_N^2}\right]\left[\sum_{n=0}^{\infty} \frac{\left[\frac{xS\sqrt{2}}{\sigma_N}\right]^{2n}}{2^{2n}(n!)^2}\right] dx$$

since the distribution has only positive values for X and

$$\int_0^{\infty} x^{2m} e^{-ax^2} dx = \frac{1\cdot 3\cdot 5\cdots(2m-1)}{2^{m+1} a^m}\sqrt{\frac{\pi}{a}}$$

Term by term integration yields

$$M = \frac{e^{-s^2}}{\sigma_N} \sum_{m=1}^{\infty} \frac{K^{2(m-1)}}{2^{2(m-1)}} \frac{\sigma_N^{m} \sqrt{\sigma_N \pi}\ 1 \cdot 3 \cdot 5 \cdots (2m-1)}{((m-1)!)^2 \sqrt{2}}$$

$$K = \frac{\sqrt{2}\, S}{\sigma_N}$$

For digital Computer Operation this series may be nested as

$$M = e^{-s^2} \sqrt{\frac{\pi}{2}}\, \sigma_N \left[\overbrace{1}^{a_0} + \overbrace{\frac{a_0 2 s^2}{2(1)^2}}^{a_1} + \overbrace{\frac{a_1 5 s^2}{2\, 2^2}}^{a_2} + \overbrace{\frac{a_2 7 s^2}{2 \cdot 3^2}}^{a_3} + \overbrace{\frac{a_3 9 s^2}{2 \cdot 4^2}}^{a_4} + \cdots \right.$$

The computer program which does this is in Appendix II.

The Second Moment for the distribution function has been evaluated in closed form as

$$E[x^2] = 2\sigma_N^2 (1 + s^2)$$

The variance or fluctuation noise power is then:

$$\sigma_R^2 = E[x^2] - (E[x])^2$$

σ_R^2 and M may be evaluated for different signal to noise power ratios.

Appendix II

The digital computer program written to compute the mean and variance of the distribution for the output of envelope detector is shown below. Sample outputs are also included in this appendix.

```
      PROGRAM SIGNOIS
C     SIGNAL VOLTAGE AND NOISE POWER FROM AN ENVELOPE DETECTOR
      DIMENSION TRM(100),EM1(90),EM2(90),XOISPR(90),SIGPR(90)
     1,DCSIG(90),EM1SQ(90),TDCSIG(90),TNOSPR(90),ERF(90)
     2,DB(90),SIGINT(90),ERFINT(90)
      POWER=0
      DO 20 I=1,90
      IF(I-10)4,4,5
    4 POWER=POWER+.01
      GO TO 10
    5 IF(I-40)6,7,7
    6 POWER=POWER+.1
      GO TO 10
    7 IF(I-60)8,9,9
    8 POWER=POWER+.5
      GO TO 10
    9 POWER=POWER+1.0
   10 SIGPR(I)=POWER
      XEGPR=-SIGPR(I)
      T=1.0
      SUM=1.0
      TRM(1)=1.0
      DO 15 N=2,100
      T=T+1.0
   15 TRM(N)=((TRM(N-1))*(SIGPR(I)*(2.0*T-1.0)))/(2.0*((T-1.0)*(1-1.0)))
     1SUM=SUM+TRM(N)
      EM1(I)=SUM*EXPF(XEGPR)*1.2533141
      EM1SQ(I)=EM1(I)*EM1(I)
      EM2(I)=2.0*(1.0+SIGPR(I))
      XOISPR(I)=EM2(I)-EM1SQ(I)
      DCSIG(I)=EM1(I)-1.2533141
      TDCSIG(I)=10.0*DCSIG(I)
      TNOSPR(I)=10.0*(XOISPR(I)+1.2871102)
      QPR=TNOSPR(I)
   20 ERF(I)=TDCSIG(I)/SQRTF(QPR)
      PRINT 21
   21 FORMAT (97H  SIG TO NOISE IN      FIRST MOMENT OUT     SECOND MOMEN
     1T OUT   DC SIGNAL VOLTAGE    NOISE POWER OUT)
      PRINT 3,(SIGPR(I),EM1(I),EM2(I),DCSIG(I),XOISPR(I),
     1I=1,90)
    3 FORMAT (5F20.8)
      PRINT 29
      PRINT 98,(SIGPR(I),TDCSIG(I),TNOSPR(I),ERF(I),I=1,90)
   98 FORMAT (4F20.8)
      PRINT 29
   29 FORMAT(1H1)
      DO 30 I=1,90
      DB(I)=10.0*(LOG10F(SIGPR(I)))
      SIGINT(I)=1.2*TDCSIG(I)
   30 ERFINT(I)=SIGINT(I)/SQRTF(TNOSPR(I))
      PRINT 31,(DB(I),SIGINT(I),ERFINT(I),I=1,90)
   31 FORMAT (3F20.8)
      END
      END
      PRINT 99,(TRM(I),I=1,100)
   99 FORMAT (F20.8)
```

SIG TO NOISE IN	FIRST MOMENT OUT	SECOND MOMENT OUT	DC SIGNAL VOLTAGE	NOISE POWER OUT
.01000000	1.25937285	2.02000000	.00625875	.43347623
.02000000	1.26581621	2.04000000	.01250191	.43770982
.03000000	1.27204366	2.06000000	.01872956	.44190492
.04000000	1.27825588	2.08000000	.02494178	.44606190
.05000000	1.28445274	2.10000000	.03113844	.45018115
.06000000	1.29063432	2.12000000	.03732022	.45426305
.07000000	1.29680070	2.14000000	.04348660	.45830796
.08000000	1.30295194	2.16000000	.04963784	.46231624
.09000000	1.30908813	2.18000000	.05577403	.46628827
.10000000	1.31520934	2.20000000	.06189524	.47022440
.20000000	1.37561349	2.40000000	.12229939	.50768752
.30000000	1.43459796	2.60000000	.18128386	.54192868
.40000000	1.49222988	2.80000000	.23891578	.57324997
.50000000	1.54857241	3.00000000	.29525831	.60192348
.60000000	1.60368509	3.20000000	.35037090	.62819443
.70000000	1.65762360	3.40000000	.40430950	.65228399
.80000000	1.71044097	3.60000000	.45712687	.67439167
.90000000	1.76218661	3.80000000	.50887271	.69469763
1.00000000	1.81290800	4.00000000	.55959390	.71336459
1.10000000	1.86264875	4.20000000	.60933465	.73053963
1.20000000	1.91145083	4.40000000	.65813673	.74635573
1.30000000	1.95935366	4.60000000	.70603956	.76093325
1.40000000	2.00639450	4.80000000	.75308040	.77438112
1.50000000	2.05260857	5.00000000	.79929447	.78679805
1.60000000	2.09802920	5.20000000	.84471510	.79827247
1.70000000	2.14268792	5.40000000	.88937382	.80888749
1.80000000	2.18661457	5.60000000	.93330047	.81871671
1.90000000	2.22983765	5.80000000	.97652335	.82782494
2.00000000	2.27238330	6.00000000	1.01906926	.83627386
2.10000000	2.31427772	6.20000000	1.06096362	.84411865
2.20000000	2.35554444	6.40000000	1.10223054	.85140945
2.30000000	2.39620702	6.60000000	1.14289292	.85819190
2.40000000	2.43628661	6.80000000	1.18297251	.86450755
2.50000000	2.47580406	7.00000000	1.22248998	.87039424
2.60000000	2.51477902	7.20000000	1.26146492	.87588648
2.70000000	2.55323017	7.40000000	1.29991607	.88101571
2.80000000	2.59117529	7.60000000	1.33786119	.88581063
2.90000000	2.62863130	7.80000000	1.37531720	.89029744
3.00000000	2.66561435	8.00000000	1.41230025	.89450014
3.50000000	2.84394883	9.00000000	1.59063473	.91195505
4.00000000	3.01248930	10.00000000	1.75917520	.92490825
4.50000000	3.17257719	11.00000000	1.91926309	.93475395
5.00000000	3.32529535	12.00000000	2.07198125	.94241085
5.50000000	3.47152788	13.00000000	2.21821378	.94849420
6.00000000	3.61200456	14.00000000	2.35869046	.95342304
6.50000000	3.74733402	15.00000000	2.49401992	.95748778
7.00000000	3.87802873	16.00000000	2.62471463	.96089319
7.50000000	4.00452416	17.00000000	2.75121006	.96378628
8.00000000	4.12719342	18.00000000	2.87387932	.96627448
8.50000000	4.24635872	19.00000000	2.99304462	.96843759
9.00000000	4.36230032	20.00000000	3.10898622	.97033594
9.50000000	4.47526359	21.00000000	3.22194949	.97201584
10.00000000	4.58545471	22.00000000	3.33215061	.97351335

SIGNAL POWER INPUT	$10(M_1-M_2)^2$	$10(\sigma_1^2+\sigma_2^2)$	$\frac{10(M_1-M_2)^2}{10(\sigma_1^2+\sigma_2^2)}$
.01000000	.06258750	17.21087255	.01508642
.02000000	.12501912	17.25320643	.03009827
.03000000	.18729563	17.29515938	.04503658
.04000000	.24941781	17.33672923	.05990235
.05000000	.31138641	17.37792175	.07469658
.06000000	.37320221	17.41874069	.08942024
.07000000	.43486595	17.45918976	.10407427
.08000000	.49637840	17.49927262	.11865960
.09000000	.55774029	17.53899290	.13317714
.10000000	.61895238	17.57835418	.14762779
.20000000	1.22299393	17.95298536	.28863963
.30000000	1.81283863	18.29539703	.42382662
.40000000	2.38915785	18.60860991	.55384454
.50000000	2.95258315	18.89534497	.67924230
.60000000	3.50370896	19.15805454	.80048738
.70000000	4.04309504	19.39895007	.91796228
.80000000	4.57126875	19.62002692	1.03201725
.90000000	5.08872714	19.82308654	1.14294025
1.00000000	5.59593897	20.00975614	1.25098491
1.10000000	6.09334652	20.18150647	1.35637284
1.20000000	6.58136728	20.33966751	1.45929873
1.30000000	7.06039557	20.48544266	1.55993448
1.40000000	7.53080397	20.61992143	1.65843265
1.50000000	7.99294473	20.74409068	1.75492923
1.60000000	8.44715102	20.85884486	1.84954598
1.70000000	8.89373818	20.96499508	1.94239234
1.80000000	9.33300478	21.06327725	2.03356713
1.90000000	9.76523352	21.15439955	2.12315985
2.00000000	10.19069261	21.23884883	2.21125188
2.10000000	10.60963617	21.31729668	2.29791747
2.20000000	11.02230541	21.39020466	2.38322458
2.30000000	11.42892922	21.45802916	2.46723563
2.40000000	11.82972511	21.52113567	2.55000808
2.50000000	12.22489963	21.58005262	2.63159500
2.60000000	12.61464921	21.63497497	2.71204555
2.70000000	12.99916069	21.68626726	2.79140537
2.80000000	13.37861187	21.73421653	2.86971693
2.90000000	13.75317205	21.77908482	2.94701986
3.00000000	14.12300250	21.82111156	3.02335122
3.50000000	15.90634731	21.99566067	3.39157914
4.00000000	17.59173195	22.12519265	3.73994799
4.50000000	19.19263094	22.22364969	4.07124109
5.00000000	20.71981248	22.30021867	4.38764276
5.50000000	22.18213777	22.36105216	4.69091195
6.00000000	23.58690462	22.41034064	4.98249328
6.50000000	24.94019915	22.45098798	5.26359164
7.00000000	26.24714628	22.48504206	5.53522450
7.50000000	27.51210057	22.51397301	5.79825992
8.00000000	28.73879320	22.53885498	6.05344502
8.50000000	29.93044624	22.56048606	6.30142782
9.00000000	31.08986218	22.57946960	6.54277414
9.50000000	32.21949486	22.59626857	6.77798125
10.00000000	33.32150415	22.61124371	7.00748857

S/N	d_b	$10(\mu_1-\mu_2)1.2$	$\frac{10(\mu_1-\mu_2)1.2}{\sqrt{10(\sigma_1^2+\sigma_2^2)}}$
	-20[illegible]00000000	.075510500	.01810370
	-1[illegible]	.15002295	.03611792
	[illegible]17960007	.22475476	.05404389
	[illegible]31029998	.29930137	.07188282
	-2.218488750	.37366270	.08963590
	-1.549019960	.44784265	.10730429
	-1.[illegible]69910013	.52183915	.12488912
	-1.[illegible]57579191	.59565408	.14239152
	-1.000000000	.66928835	.15981257
	-.[illegible]98970004	.74274285	.17715335
	-.[illegible]22872345	1.4075927[illegible]	.34636756
	-.[illegible]97948009	2.175406[illegible]	.50829194
	-.[illegible]31029996	2.86698942	.66461345
	-.[illegible]21848750	3.54309977	.81509076
	-.[illegible]54901960	4.20445073	.96058004
	-.[illegible]96910013	4.85171405	1.10155474
	-.[illegible]45757791	5.48552250	1.23842070
	.000000000	6.10647257	1.37152830
	.413926[illegible]	6.71512677	1.50118189
	.791812[illegible]	7.31201582	1.62764741
	1.139433[illegible]	7.89764074	1.75115847
	1.467288[illegible]	8.47247469	1.87192138
	1.760912[illegible]	9.03696476	1.99011918
	2.041199[illegible]	9.59153367	2.10591508
	2.304489[illegible]	10.13658123	2.21945517
	2.552725[illegible]	10.67244881	2.33087081
	2.787536[illegible]	11.19960569	2.44023056
	3.010299[illegible]	11.71828023	2.54778182
	3.222192[illegible]	12.22883115	2.65350225
	3.424226[illegible]	12.73156241	2.75758096
	3.617278[illegible]	13.22676649	2.85986950
	3.802112[illegible]	13.71471509	2.96068276
	3.979400[illegible]	14.19567014	3.06000969
	4.149733[illegible]	14.66987955	3.15791400
	4.313637[illegible]	15.13757905	3.25445466
	4.471580[illegible]	15.59899282	3.34968644
	4.623979[illegible]	16.05433424	3.44366031
	4.771212[illegible]	16.50380646	3.53642383
	5.440680[illegible]	16.94760300	3.62802146
	6.020599[illegible]	19.08761677	4.06989497
	6.532125[illegible]	21.11010234	4.48793758
	6.989700[illegible]	23.03115713	4.88548931
	7.403626[illegible]	24.86377498	5.26517131
	7.781512[illegible]	26.61856533	5.62909434
	8.129133[illegible]	28.30428554	5.97899194
	8.450980[illegible]	29.92823898	6.31630997
	8.750612[illegible]	31.49657553	6.64226939
	9.030899[illegible]	33.01452068	6.95791191
	9.294189[illegible]	34.48655183	7.26413403
	9.542425[illegible]	35.91653549	7.56171338
	9.777236[illegible]	37.30783461	7.85132897
	10.000000000	38.66339383	8.13357750
		39.98580738	8.40898628

APPENDIX III

FILTER CHARACTERISTICS OF AN INTEGRATOR

The impulse response of an ideal integrator which integrates for a time interval T is shown as a solid line in Fig. A. /17/

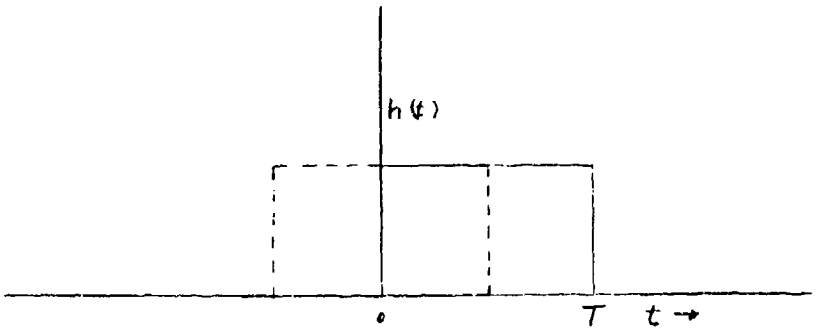

Impulse response of an ideal integrator.

Figure III-A

To obtain the transfer characteristics in the frequency domain translate the coordinates an amount T/2, shown as dotted in Fig. A. Transform this to the frequency domain.

$$H'(\omega) = \int_{-\infty}^{\infty} \frac{1}{T} e^{-j\omega t}\, dt \qquad -T/2 \leq t \leq T/2$$

$$H'(\omega) = \frac{1}{T} \int_{-T/2}^{T/2} e^{-j\omega t}\, dt$$

$$H'(\omega) = \frac{\sin \omega T/2}{\omega T/2} = \frac{\sin \pi f T}{\pi f T}$$

A delay in the time domain of T/2 seconds is manifest as a phase shift in the frequency domain of $e^{-j\omega T/2}$. Hence

$$H(\omega) = e^{-j\omega T/2} \frac{\sin \omega T/2}{\omega T/2}$$

$$= e^{-j\omega T/2} \frac{\sin \pi f T}{\pi f T}$$

The power output of such an integrator would be

$$P_o = \int_{-\infty}^{\infty} |H(\omega)|^2 G(\omega)\, df$$

where G(W) is the power spectral density of the input signal.

The power output of the integrator becomes

$$P_o = \int_{-\infty}^{\infty} \left| e^{-j\omega T/2} \frac{\sin \pi f T}{\pi f T} \right|^2 G(\omega)\, df$$

$$= \int_{0}^{\infty} \frac{\sin^2 \pi f T}{\pi f T} G(\omega)\, df$$

for one sided frequency spectrum.

For this problem T = 2 x 10^{-3} seconds. The frequency of the first zero is then

$$\pi f T = \pi$$

$$f = \frac{1}{T} = 500 \text{ c.p.s.}$$

For any one of those three channels which for any instant contain noise only the power spectral density is as shown in Fig. 13 from /11/

$$P_{in} = \int_0^{500} G(\omega)\, df = \frac{1}{2}(2C \times 500) = 500C \text{ watts}$$

From the Rayleigh distribution, the variance or fluctuation noise power is $.429\sigma N^2$.

Then $$.429\sigma_N^2 = \frac{1}{2}(2C \times 500)$$

$$C = \frac{.429\sigma_N^2}{500}$$

$$G(\omega) = -\frac{2Cf}{500} + 2C = 2C\left[-\frac{f}{500} + 1\right]$$

$$= (2)\frac{.429\sigma_N^2}{250{,}000} f + \frac{(2)\,.429\sigma_N^2}{500}$$

There will always be three channels of noise power $.429\sigma N^2$ and the noise power from the signal channel going

into the integrator which will add directly since the noise from different parts of the spectrum are not coherent. The noise power in the signal channel will be increasing with the increasing signal power. Thus the noise power may be considered as four channels of noise power plus the increased noise power in the signal channel due to the signal times noise products. This increase may be closely approximated by curve fitting techniques applied to Fig. III-B. By linear regression the increase in noise power is

$$\Delta P = .571\left[1 - e^{-.62X}\right]$$

where X is the signal to noise power ratio.

This increase in noise power is essentially flat over half the original bandwidth of the noise input to the detector. Thus the Noise Power Spectral Density into the integrator will be

$$G(\omega) = \frac{(4)(2)(.429)\sigma_N^2}{500}\left[-\frac{f}{500} + 1\right] + .571\left[1 - e^{-.62X}\right]$$

and the power output of the integrator is

$$P_o = \int_0^{500} K\left[-\frac{f}{500} + 1\right] + .571\left[1 - e^{-.62X}\right] \frac{\sin^2 \pi f T}{(\pi f T)^2}\, df .$$

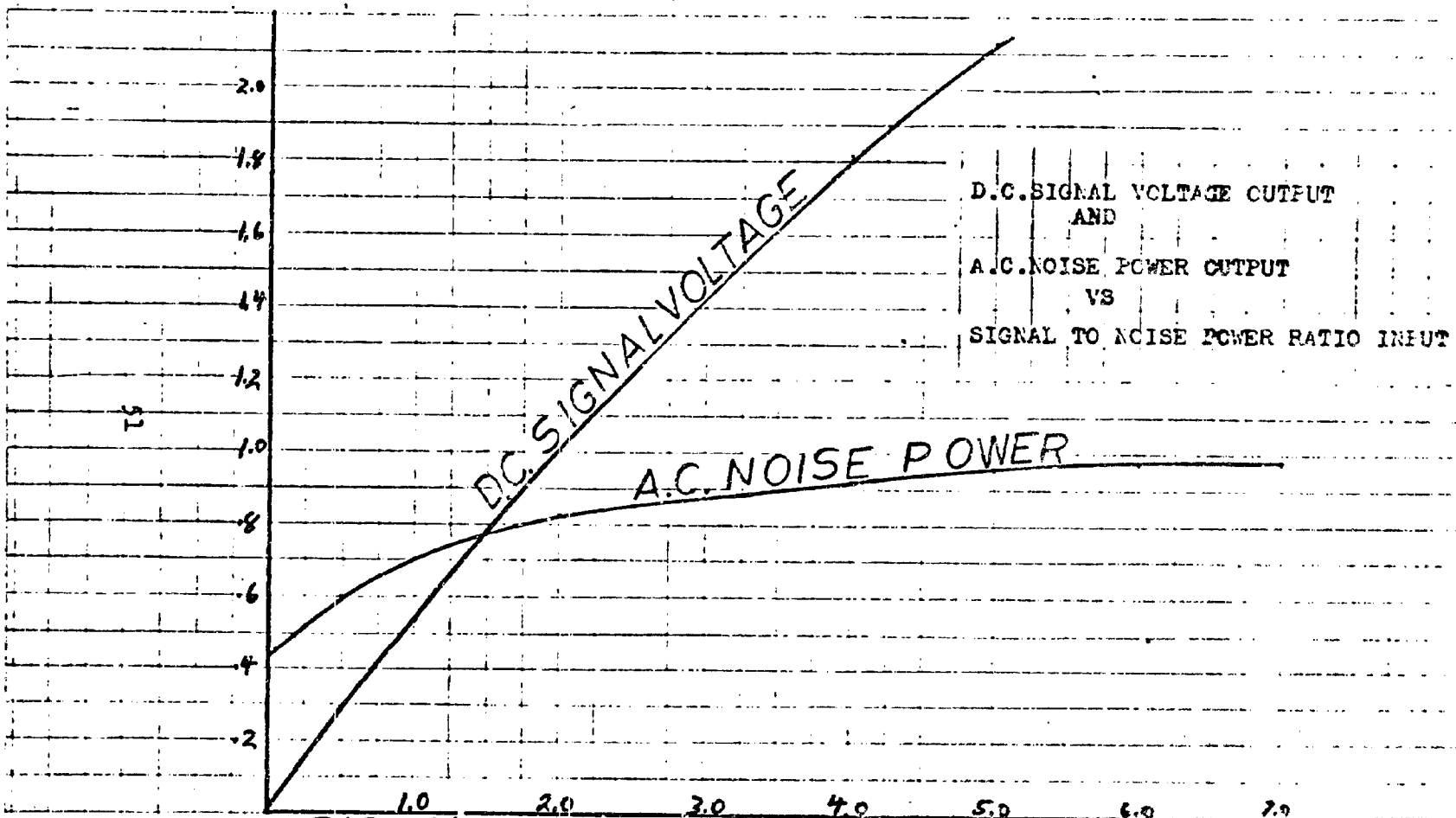

D.C.SIGNAL VOLTAGE OUTPUT
AND
A.C.NOISE POWER OUTPUT
VS
SIGNAL TO NOISE POWER RATIO INPUT

Fig III-8

The power spectral density input to the integrator will be as shown in Fig. III-C.

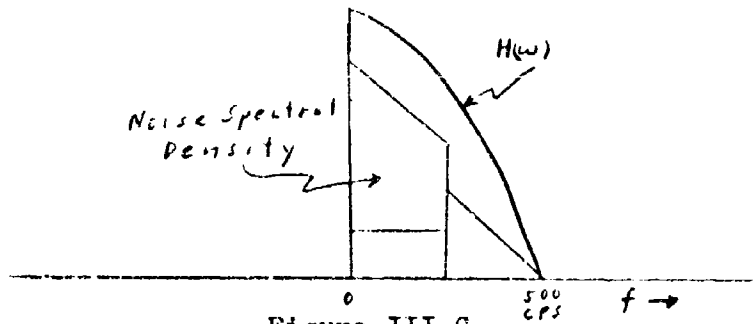

Figure III-C

In order to obtain a tractable model the noise power spectral density will be assumed to be flat from zero to B/2 cycles per second with a total noise power equal to the original noise power. The noise power out of the detector then is

$$P_o = \int_{-\infty}^{\infty} \frac{N}{2} |H(\omega)|^2 \, df$$

$$= \frac{N}{2} \int_{-\pi/2}^{\pi/2} \frac{\sin^2 \pi f T}{(\pi f T)^2} \, df$$

Transforming variables

$$P_o = \frac{N}{2} \int_{-\pi/2}^{\pi/2} \frac{\sin^2 \theta}{\theta} \, d\theta = .774 N$$

This modifies the error rate to be

$$P_e = \frac{1}{2}\left[1 - Erf \frac{10(M_1 - M_2)}{\sqrt{(.774)(10)(\sigma_1^2 + 30\sigma_2^2)}}\right]$$

$$= \frac{1}{2}\left[1 - Erf \frac{10(M_1 - M_2)\,1.2}{\sqrt{10(\sigma_1^2 + 30\sigma_2^2)}}\right].$$

APPENDIX IV

The analysis of the QFM demodulator assumed a square pulse shape for each bit transmitted as shown in Fig. 1. The pulse transmitted is shown in Fig. 2. In order to bridge the gap between the model and the actual modulator the following conversion proceedure was applied.

The power in a constant unmodulated carrier of amplitude A is $A^2/2$.

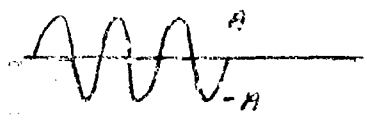

$P_c = \frac{A^2}{2}$

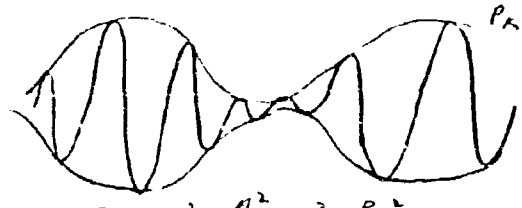

$P_{mc} = 3/2 \cdot \frac{A^2}{2} = \frac{3}{8} \frac{P_K^2}{2}$

The cosine squared pulse which is the output of the rectifier is obtained from an input to the rectifier of a waveform like a carrier 100 per cent modulated by a sine wave. The power in this signal is 3/2 $\frac{A^2}{2}$. In terms of the peak voltage of the modulated carrier

$$P_{mc} = \frac{3}{2} \cdot \frac{1}{2} \left(\frac{P_K}{2}\right)^2 = \frac{3}{2} \frac{P_K^2}{8} = \frac{3}{8} \frac{P_K^2}{2}$$

The "mark" or "space" decision is based on the polarity of the integrator output after 2 millisiconds of integration.

The output of the integrator for the modulated input is

$$\frac{1}{\pi/2} \int_{-\pi/4}^{\pi/4} P_K \cos^2\theta \, d\theta = .82 P_K$$

The amplitude of a constant carrier pulse for an equivalent voltage output of the intigrator would be .82 PK.

The power in this carrier is

$$P_{CR} = \frac{(.82 P_R)^2}{2} = \frac{.6724 P_R^2}{2}$$

The power in a constant carrier signal which will produce the same output at the integrator as a modulated carrier with a power per bit of P_B is

$$P_{EQ} = P_B \left[\frac{.6724 \frac{P_R^2}{2}}{.375 \frac{P_R^2}{2}} \right]$$

$$= 1.78 P_B$$

Since all signal to noise ratios are referred to a noise power of one, the Signal Power is the signal to noise ratio, and

$$10 \log P_{EQ} = 10 \log 1.78 + 10 \log P_B$$

$$S/N_{EQ} = S/N_B + 2.53 \text{ db}$$

Thus 2.53db should be added to the signal power per bit as measured.

To refer the model to the measured signal power 2.53db must be subtracted from the theoretical noise power.

APPENDIX V

ERROR DETECTION INSTRUMENTATION

Some means of detecting errors was necessary in order to obtain an error count. Since the output data was digital, a digital system was used for error detection. Engineered Electronics building blocks were arranged as shown in the diagram below.

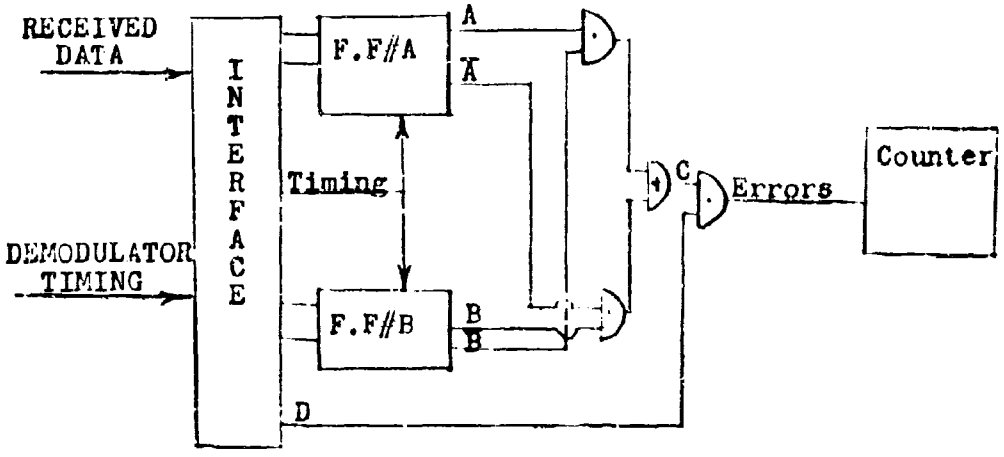

Flip flop A assumed the state corresponding to the "Mark" or "Space" data received. Flip flop B assumed the state of the transmitted data. The outputs were gated according to the following equation.

$$C = (A \cdot \overline{B}) - (\overline{A} \cdot B)$$

$$\text{Error} = (C \cdot D)$$

D was derived from the interface timing circuits.